AD-A235 007

AeroChem TP-495

AFOSR-TR- 91 0229

COMPUTER MODELING OF SOOT FORMATION COMPARING FREE RADICAL AND IONIC MECHANISMS

(A Collaborative Effort Among AeroChem, Penn State, and Iowa State)

DTIC
ELECTE
APR 3 1991
C

H. F. Calcote and Robert J. Gill

AEROCHEM RESEARCH LABORATORIES, INC.
P.O. Box 12
Princeton, New Jersey 08542

February 1991

Final Report for Period 1 October 1987 to 30 September 1990

Approved for Public Release
Distribution Unlimited

Prepared for

AIR FORCE OFFICE OF SCIENTIFIC RESEARCH
Bolling Air Force Base
Washington, DC 20332

91 4 16 166

UNCLASSIFIED
SECURITY CLASSIFICATION OF THIS PAGE

REPORT DOCUMENTATION PAGE

Form Approved OMB No. 0704-0188

1a. REPORT SECURITY CLASSIFICATION Unclassified	1b. RESTRICTIVE MARKINGS
2a. SECURITY CLASSIFICATION AUTHORITY	3. DISTRIBUTION/AVAILABILITY OF REPORT Approved for public release; distribution is unlimited
2b. DECLASSIFICATION/DOWNGRADING SCHEDULE	
4. PERFORMING ORGANIZATION REPORT NUMBER(S) TP-495	5. MONITORING ORGANIZATION REPORT NUMBER(S)
6a. NAME OF PERFORMING ORGANIZATION AeroChem Research Labs., Inc. — 6b. OFFICE SYMBOL (If applicable): NA	7a. NAME OF MONITORING ORGANIZATION AFOSR/NA
6c. ADDRESS (City, State, and ZIP Code) P.O. Box 12 Princeton, NJ 08542	7b. ADDRESS (City, State, and ZIP Code) Building 410, Bolling AFB DC 20332-6448
8a. NAME OF FUNDING/SPONSORING ORGANIZATION AFOSR/NA — 8b. OFFICE SYMBOL (If applicable): NA	9. PROCUREMENT INSTRUMENT IDENTIFICATION NUMBER F49620-88-C-0007
8c. ADDRESS (City, State, and ZIP Code) Building 410, Bolling AFB DC 20332-6448	10. SOURCE OF FUNDING NUMBERS PROGRAM ELEMENT NO.: 61102F — PROJECT NO.: 2308 — TASK NO.: A2 — WORK UNIT ACCESSION NO.:

11. TITLE (Include Security Classification)
(U) Computer Modeling of Soot Formation Comparing Free Radical and Ionic Mechanisms

12. PERSONAL AUTHOR(S)
H.F. Calcote and R.J. Gill

13a. TYPE OF REPORT	13b. TIME COVERED	14. DATE OF REPORT (Year, Month, Day)	15. PAGE COUNT
Final	FROM 10/1/87 TO 9/30/90	1991 February 28	44

16. SUPPLEMENTARY NOTATION

17. COSATI CODES			18. SUBJECT TERMS (Continue on reverse if necessary and identify by block number)
FIELD	GROUP	SUB-GROUP	Soot Formation; Ionic Mechanism; Thermodynamics; Ion-Molecule Reactions; Ion Electron Recombination; Ionic Diffusion

19. ABSTRACT (Continue on reverse if necessary and identify by block number)

A collaborative effort among AeroChem Research Laboratories Inc., Pennsylvania State University, and Iowa State University has been pursued to compare the relative importance of the free radical and the ionic mechanisms of soot formation. A detailed ionic reaction mechanism was developed; the rate coefficients were obtained from the literature or estimated; ambipolar diffusion and ion-electron recombination coefficients were calculated; and thermodynamic data for the ions were either compiled from the literature or calculated. Computer runs were made at Penn State using our ionic mechanism to simulate the well-documented sooting acetylene/oxygen/argon flat flame at a pressure of 2.67 kPa and a linear flow rate of 50 cm/s. The calculated peak ion concentrations were consistent with experimental peak concentrations, but the calculated ion profiles appeared much earlier in time and decayed very rapidly compared to the experimental ion profiles. This was suspected to be dependent upon the calculated neutral species profiles from the free radical mechanism for small neutrals, which are required to form chemiions. These are not in good agreement
(over)

20. DISTRIBUTION/AVAILABILITY OF ABSTRACT	21. ABSTRACT SECURITY CLASSIFICATION
☐ UNCLASSIFIED/UNLIMITED ☑ SAME AS RPT. ☑ DTIC USERS	Unclassified

22a. NAME OF RESPONSIBLE INDIVIDUAL	22b. TELEPHONE (Include Area Code)	22c. OFFICE SYMBOL
Julian M. Tishkoff	(202) 767-0465	AFOSR/NA

BLOCK 19 (Continued)

with experiment. Thus computer runs were made at Iowa State using experimental neutral species profiles rather than calculated values, and our suspicions were confirmed.

In another type of analysis, comparison of the rate of carbon species growth in the free radical and ionic mechanisms, using experimental profiles and available rate coefficients, indicates that the two rates are very close. The comparison is limited to small species because profiles for large neutral species are unavailable; they are apparently below the detection limit of the experiments. This implies that the ion carbon growth flux is greater than the neutral species carbon growth flux.

Experimental data previously obtained were analyzed to demonstrate that the rate of ion growth for ions up to very large ions is comparable to the rate of formation of soot particles.

Recommendations are made for future work to understand the mechanism of soot nucleation. The major need relative to the free radical mechanism is for experimental profile data for much larger neutral and radical species than are currently available. The major need relative to the ionic mechanism is for experimental profiles of negative ions.

TABLE OF CONTENTS

Accession For
NTIS GRA&I ☑
DTIC TAB ☐
Unannounced ☐
Justification
By
Distribution/
Availability Codes
Dist | Avail and/or Special
A-1

LIST OF FIGURES

I. INTRODUCTION

This is the final report on this program which was a collaborative effort among AeroChem (Principal Investigator: H. F. Calcote), Penn State (Principal Investigator: M. Frenklach) and Iowa State (Principal Investigator: R. C. Brown). The ultimate objective has been to develop a quantitative model of soot formation in flames that is consistent with experimental data. The specific objectives of this collaborative three-year study were: (1) to delineate the relative importance of the neutral free radical and ionic mechanisms of soot formation in flames; (2) to determine the optimum model of the total soot formation process based upon current knowledge; and (3) to recommend how to improve the model and the additional experiments necessary to clarify any discrepancies.

Professor Robert Brown, Iowa State University, was added to the program in the last year as a collaborator via a subcontract from AeroChem, with funds which were added to this program for that purpose. He brought to the program previous experience in developing a code for modeling ionic reactions in flames[1,2] involving the solution of the stiff equations involved in such reactions. Brown's code was originally developed to include ions as well as neutrals. It handles non-Arrhenius temperature coefficients in the ion-molecule rate coefficients; in the code used by Frenklach this has been a problem. The diffusion coefficient for ions and electrons is included via Poisson's equation; in the code used by Frenklach this is handled in an indirect way. Brown's code also permits running the neutral species separately and then using these results as input to the ion code. This allows the use of experimental species profiles as input, so that only the part of the mechanism of interest can be studied. As we will see this makes a major difference. The validity of the test of the ionic mechanism is no longer dependent upon the free radical mechanism of small species. We have already spent considerable effort in developing this part of the mechanism and have not yet had a good test of it. As we will see, the free radical mechanism is not consistent with the observed small species in the flame. A more complete set of experimental neutral species profiles was made available to us by Vovelle.[3]

The AeroChem and Iowa State effort are presented in this report; the Penn State effort is covered in their companion report.[4] AeroChem is responsible for development of the thermodynamics, diffusion coefficients, reaction mechanism, and reaction rate coefficients for the ionic mechanism. There were no previous sets of data on the ionic mechanism to draw upon when we initiated this program; two papers were subsequently published by Brown and Eraslan,[1,2] in which they calculated the concentrations of ions in both stoichiometric and fuel rich flames; their calculations compared favorably with experiments. For the sooting flames we model in this program, it has been necessary not only to construct the ionic mechanism and identify the rate coefficients but also to develop neutral mechanisms and to organize data for odd number neutral carbon compounds. Such species were not generally utilized in the free radical mechanisms of soot formation. Odd carbon neutral species, however, play a significant role in the ionic mechanism and are observed in relatively large concentrations in sooting flames.

The computer modeling results are compared with the well-documented acetylene/oxygen flame (the "standard flame") burning on a flat flame burner at a pressure of 2.67 kPa (20 Torr) and a linear flow rate of 50 cm/s in the unburned gases. In our previous AFOSR contract work,[5–7] we duplicated the Bittner and Howard[8] burner used to obtain neutral species concentrations and we measured ion concentration profiles with this burner so that the ion profiles and the neutral profiles would be from the same system. We also compared the data obtained by a number of other researchers on very nearly the same flame; we previously presented the results of this comparison[5] which showed amazing agreement among several laboratories. This data base forms an excellent experimental standard with which to compare the computer modeling results.

Preliminary computer experiments were carried out for a shock tube to obtain some feel of how the ionic mechanism performed in the computer program, and to work out some of the details of the mechanism. This is not a good system in which to compare the two mechanisms because there are no ion profile data. Further, at the time of this preliminary work the ionic mechanism was in a very crude state of development so the results are of little value in so far as comparing the ionic and free radical mechanisms. Frenklach has, however, chosen[4] to interpret these results as indicating "that the ionic mechanism produces polycyclic aromatic hydrocarbons (PCAH) at a significantly lower rate than does the mechanism composed of only reactions of neutral species." Not only is this a premature conclusion, but more seriously, Frenklach continues to misinterpret the ionic mechanism, in spite of many personal explanations.

The basic premise of the ionic mechanism is that ions grow to a very large size to become incipient soot particles or to be neutralized and produce large neutrals, 500 to 1,000 u, which grow to become incipient soot particles. Frenklach interprets the ionic mechanism as producing small PCAH neutrals and then compares the concentration of such species as benzene and acenaphthalene produced by the free radical and ionic mechanisms. Frenklach states in his abstract,[4] "the formation of polycyclic aromatic hydrocarbons, the precursors to soot, via the ionic reaction pathway is slower than via the pathway involving neutral species"; neutral polycyclic aromatic hydrocarbons do not play a role (except as by-products) in the ionic mechanism. The production of such small neutrals is a result of ion-molecule reactions which remove ions from the main stream, and are thus unwanted by-products. The basic question which should be addressed is what is the flux of carbon (atoms) through the ionic reaction scheme vs. through the radical reaction scheme of leading to soot; neutrals for the free radical mechanism and ions for the ionic mechanism.

At the present state of this research, it would be premature to decide between the two mechanisms. We present some new evidence which favors the ionic mechanism over the free radical mechanism. Reference 9 summarizes some of the earlier evidence for the ionic mechanism. There is no equivalent evidence for the free radical mechanism. Consistent with the contract objectives, we identify work which needs to be done to understand the relative role of ions and neutrals in soot inception.

II. STATEMENT OF WORK

A. Organize relevant data on ion-molecule reactions, thermochemistry, electron attachment, ion recombination, and ion and electron diffusion to be used in the computer code simulation by Penn State.

B. Determine the hydrogen atom concentration in the "well-studied" C_2H_2/O_2 flame and determine if this concentration exceeds the thermal equilibrium concentration.

C. Analyze the computer simulation data obtained by Penn State and compare the results with available experimental data to determine the major chemical pathways to incipient soot and to simplify the computer model.

D. Organize relevant data on the elementary steps involved in the growth of incipient soot to soot particles, including growth by molecular addition, coagulation, and oxidation.

E. Analyze the computer simulation data obtained by Penn State using the extended model and compare the results with available experimental data to determine the major pathways to particulate soot and to determine how to alter the model to make it more in conformity with experimental results.

F. Review the literature and choose flame experiments with which to compare the model developed above.

G. Analyze the computer simulation data obtained by Penn State and compare the results with the experimental data to determine the general applicability of the model and to recommend what is required to improve the model and what additional experiments are necessary to clarify any discrepancies.

The Statement of Work for the subcontract with Brown at Iowa State was:

A. Incorporate reaction mechanism and thermochemical data developed at AeroChem Research Laboratories in the TRANSEQI computer code.

B. Assess the utility of determining ambipolar diffusion by numerical solution of the Poisson equation using a sample ion model.

C. Perform baseline simulations of a test flame.

D. Perform numerical simulations of the standard acetylene/oxygen flame.

III. THERMODYNAMICS

The required thermodynamic data for most of the ions and some of the neutral species were either collected from the literature or calculated. Available compilations of data for ions, e.g., Refs. 10–12 contain very few odd number carbon atom ions; experimentally these species dominate in the flame mass spectra. The compilations also do not include isomers, which are of interest. Thermodynamic data for these species were generated as described below.

Data on a number of species, e.g., vinyl radical, C_3H_2 isomers, $C_2H_3^+$ isomers, $C_3H_3^+$ isomers, $C_7H_5^+$, $C_8H_7^+$, $C_{10}H_9^+$, $C_{13}H_8^+$, and several larger ions, were recalculated, based upon new thermodynamic information. New calculations were made for 94 ions and their isomers. The results for many of these were presented in Ref. 13 and will not be included here.

The thermodynamic quantities, $C_p°$ and $S°$ for hydrocarbons and hydrocarbon ions, were calculated, when sufficient information was available from vibrational frequencies and moments of inertia using statistical mechanical methods, or when not available, following Benson's thermochemical methods of group additives. Enthalpies of formation at 298 K, $\Delta H_f° 298$, were obtained either directly from the literature or calculated from experimental proton affinities and the corresponding neutral molecule's enthalpy of formation.

Unfortunately, there are several neutral molecules for which the thermodynamic data are uncertain. This is, for example, the case with diacetylene, an important reactant in the ionic mechanism. The available heats of formation at 298 K range from 439 to 473 kJ/mol.[14–18] We have used 440 kJ/mol[14] because the data in this reference were used previously in several thermochemical calculations with large ions. This uncertainty will be manifest in the flame simulations when rates for reverse chemical reactions are calculated from thermodynamics and forward reaction rate coefficients. For a few cases, such as for the cyclopropenyl ion, $C_3H_3^+$, another important participant in the ionic mechanism, there was sufficient experimental information to employ the more accurate statistical mechanical methods to calculate $C_p°$ and $S°$.

The inaccuracy of thermodynamic data continues to contribute a major question in any reaction kinetics scheme.

IV. REACTION MECHANISM AND REACTION COEFFICIENTS

The overall mechanism is shown in Fig. 1. The ionic path starts when electronically excited CH (CH^*) reacts with an oxygen atom to produce HCO^+, which, through a series of ion-molecule reactions, produces $C_3H_3^+$, an ion which is observed in large concentrations in fuel rich and sooting flames. This ion then reacts with any of six small neutral species, indicated in Fig. 1, to produce larger ions which continue to grow through a series of ion-molecule reactions with the same six species producing larger and larger ions. To simplify the number of reactions that have to be handled we have only considered C_2H_2, C_4H_2 and C_3H_4 in the reaction set. Simultaneously as the ions grow, they are neutralized at a rate which increases with increasing mass, producing "neutral by-products," polycyclic aromatic hydrocarbons, that, of course, can continue to grow to soot through the "free radical mechanism." These neutral reactions have not yet been incorporated into the mechanism; they probably play only a small role except for very large molecules.

The complete reaction mechanism with reaction rate coefficients and free energies of reaction at 1750 K is presented in Table I as it presently exists. This set of 128 reactions has been chosen from about 400 reactions.

In developing this mechanism only ionic species which have been observed in sooting flames have been included and all ions observed in the flame have been accounted for. This is a more stringent constraint than has ben applied to the free radical mechanism.

A. EXCITED STATE/CHEMIIONIZATION

Specific reactions which produce excited CH, (CH^*), important in the chemiionization process, and the subsequent chemiionization reactions are presented in Table I. A. Probably the two most important reactions in this set (a sensitivity analysis has yet to be analyzed), are Reactions (3) and (8). The rate coefficient for Reaction (3) was estimated by W. Gardiner[19] and the rate coefficient for Reaction (8) was measured by Cool relative to the rate coefficient for Reaction (7).[20] The reaction coefficient for Reaction (7) is from a bimolecular quantum RRK theory calculation by Westmoreland which is in agreement with experiment.[3,14]

B. ION-MOLECULE REACTIONS

When available, experimental rate coefficients were used, but these are available only for small ions. In general, experimental rates are very close to the rate calculated by the average dipole orientation, ADO, theory[16]

$$k = \frac{2\pi e}{\mu^{1/2}} \left[\alpha^{1/2} + C\mu_D \left(\frac{2}{\pi kT} \right)^{1/2} \right] \qquad (1)$$

where, μ is the reduced mass, α is the polarizability of the neutral reactant, C is a locking constant determined from experimental data, and μ_D is the dipole moment of the neutral reactant. For

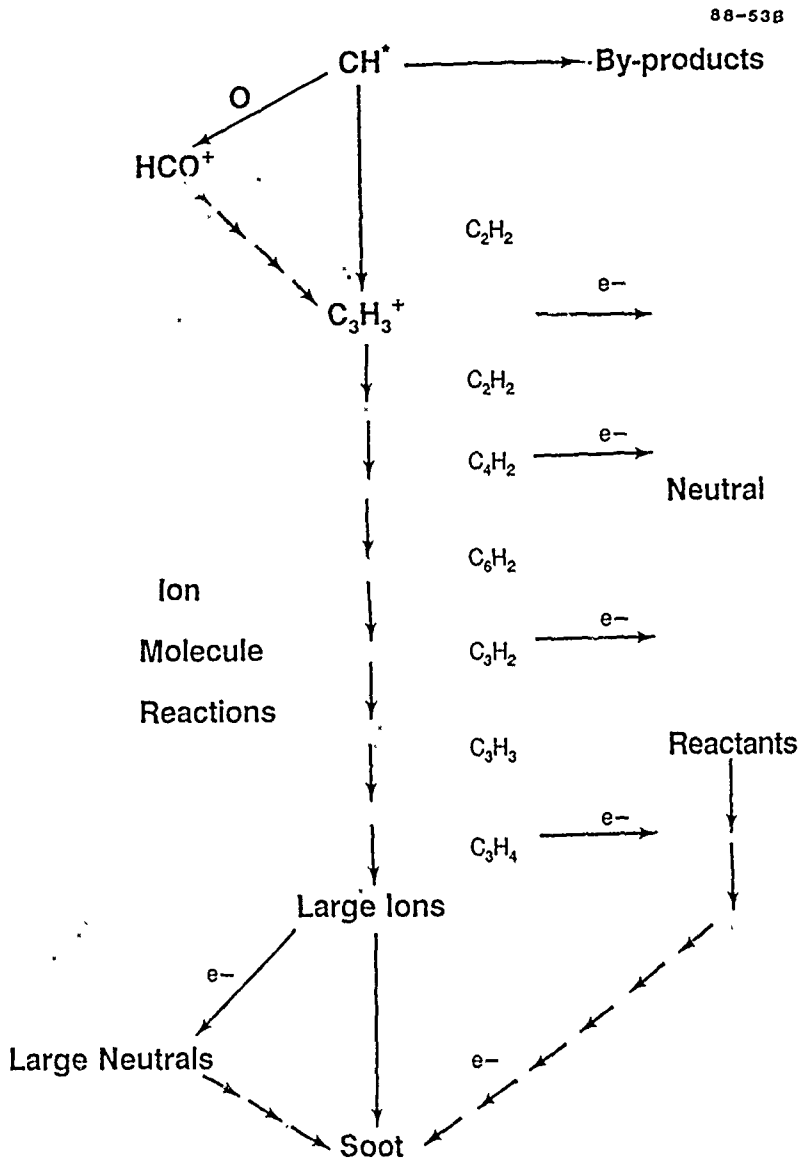

FIGURE 1 IONIC MECHANISM OF SOOT FORMATION

TABLE I
REACTION MECHANISM AND REACTION RATE COEFFICIENTS FOR THE IONIC MECHANISM OF SOOT FORMATION

$$k = A\,T^{n}\,e^{-E/RT}\ (K,\ kJ,\ moles,\ cm^2,\ s)$$

A. EXCITED STATE/CHEMIIONIZATION REACTIONS

No.	REACTION	A	n	E
1	$C_2 + OH \rightarrow CH^* + CO$	3.4E+12	0	0
2	$C_2H + O \rightarrow CH^* + CO$	7.1E+11	0	0
3	$C_2H + O_2 \rightarrow CH^* + CO_2$	4.5E+15	0	105
4	$CH^* + M \rightarrow CH + M$	4.0E+10	0.5	0
5	$CH^* + O_2 \rightarrow CH + O_2$	2.4E+12	0.5	0
6	$CH^* \rightarrow CH$	1.7E+06	0	0
7	$CH + O \rightarrow HCO^+ + e$	1.4E+10	0	2
8	$CH^* + O \rightarrow HCO^+ + e$	4.8E+14	0	0

B. ION-MOLECULE REACTIONS[a]

No.	REACTION	ΔG(1750)	Forward Rate Coefficient, k, cm^3/mole/s 500	1000	1500	2000
1	$CH_3^+ + C_2H_2 = H_3C_3^+ + H_2$	-213.1	8.3E+14			
2	$CH_3^+ + C_4H_2 = H_5C_5^+$	-290.9	1.0E+15			
3	$H_3O^+ + C_3H_2 = H_3C_3^+ + H_2O$	-253.9	8.5E+14			
4	$C_2H_3^+ + C_2H_2 = C_4H_5^+$	-96.7	7.1E+14			
5	$C_2H_3^+ + C_4H_2 = C_6H_5^+$	-141.3	8.2E+14			
6	$HCO^+ + CH_2 = CH_3^+ + CO$	-203.1	5.2E+14			
7	$HCO^+ + H_2O = H_3O^+ + CO$	-107.6	1.9E+15			
8	$HCO^+ + C_2H_2 = C_2H_3^+ + CO$	-75.0	6.9E+14			
9	$HCO^+ + C_2H_3 = H_3C_3^+ + OH$	32.2	1.5E+13	2.4E+13	3.3E+13	4.1E+13
10	$HCO^+ + C_3H_2 = H_3C_3^+ + CO$	-361.5	7.5E+14			
11	$HCO^+ + C_3H_4 = H_3C_3^+ + H_2 + CO$	-271.0	7.9E+14			
12	$C_3H_3^+ + M = H_3C_3^+ + M$	-64.6	5.0E+14			
13	$C_3H_3^+ + C_2H_2 = C_5H_2H^+ + H_2$	6.8	6.5E+14	6.5E+14	6.5E+14	4.5E+14
14	$C_3H_3^+ + C_2H_2 = H_5C_5^+$	-135.6	6.5E+14			
15	$C_3H_3^+ + C_4H_2 = C_5H_2H^+ + C_2H_2$	0.0	7.4E+14	7.4E+14	7.4E+14	5 1E+14
16	$C_3H_3^+ + C_4H_2 = C_7H_4H^+$	-67.3	7.4E+14			
17	$C_4H_5^+ + C_2H_2 = C_6H_5^+ + H_2$	-37.8	6.2E+14			
18	$C_5H_2H^+ + C_2H_2 = C_7H_4H^+$	-67.2	6.0E+14			
19	$C_5H_2H^+ + C_3H_4 = C_6H_5^+ + C_2H_2$	-178.9	6.5E+14			

No.	REACTION	ΔG(1750)	Forward Rate Coefficient, k, cm^3/mole/s 500	1000	1500	2000
20	$H_5C_5^+ + C_2H_2 = H_7C_7^+$	-35.7	6.0E+14			
21	$H_5C_5^+ + C_4H_2 = H_7C_9^+$	-30.4	6.5E+14			
22	$C_6H_5^+ + CH_2 = C_7H_4H^+ + H_2$	-202.5	4.7E+14			
23	$C_6H_5^+ + C_2H_2 = C_8H_7^+$	-42.0	5.8E+14			
24	$C_7H_4H^+ + H_2 = H_7C_7^+$	-101.0	8.9E+14			
25	$C_7H_4H^+ + C_2H_2 = C_9H_7^+$	-17.6	5.7E+14			
26	$C_7H_4H^+ + C_2H_2 = H_7C_9^+$	-98.7	5.7E+14			
27	$H_7C_7^+ + C_2H_2 = H_7C_9^+ + H_2$	2.3	5.7E+14	5.7E+14	5.7E+14	4.6E+14
28	$H_7C_7^+ + C_2H_2 = C_9H_7^+ + H_2$	83.4	7.7E+06	5.2E+10	1.2E+12	5.8E+12
29	$C_8H_7^+ + C_2H_2 = C_{10}H_9^+$	-49.3	5.6E+14			
30	$C_8H_7^+ + C_2H_2 = H_9C_{10}^+$	81.0	5.6E+14			
31	$C_8H_7^+ + C_3H_4 = H_9C_{11}^+ + H_2$	-19.9	6.0E+14			
32	$C_9H_7^+ + M = H_7C_9^+ + M$	-81.1	4.5E+14			
33	$C_9H_7^+ + C_2H_2 = C_{11}H_8H^+$	-80.2	5.6E+14			
34	$H_7C_9^+ + C_2H_2 = C_{11}H_8H^+$	0.9	5.6E+14			
35	$H_7C_9^+ + C_2H_2 = H_9C_{11}^+$	94.1	5.6E+14			
36	$C_9H_7^+ + C_3H_4 = C_{10}H_9^+ + C_2H_2$	-185.3	5.9E+14			
37	$C_9H_7^+ + C_3H_4 = H_9C_{10}^+ + C_2H_2$	-54.9	5.9E+14			
38	$C_9H_7^+ + C_4H_2 = C_{13}H_6H_3^+$	-209.9	5.8E+14			
39	$H_7C_9^+ + C_4H_2 = C_{13}H_6H_3^+$	-128.8	5.8E+14			
40	$C_{10}H_9^+ + C_2H_2 = C_{12}H_9^+ + H_2$	-23.0	5.5E+14			
41	$H_9C_{10}^+ + C_2H_2 = C_{12}H_9^+ + H_2$	-153.4	5.5E+14			
42	$H_9C_{10}^+ + C_2H_2 = H_9C_{12}^+ + H_2$	-10.5	5.5E+14			
43	$C_{10}H_9^+ + C_2H_2 = H_9C_{12}^+ + H_2$	119.8	2.7E+06	7.8E+09	1.1E+11	4.2E+11
44	$H_9C_{11}^+ + M = C_{11}H_8H^+ + M$	-93.2	4.5E+14			
45	$C_{11}H_8H^+ + C_2H_2 = C_{13}H_6H_3^+ + H_2$	-122.8	5.5E+14			
46	$C_{11}H_8H^+ + C_2H_2 = C_{13}H_8H^+ + H_2$	86.0	2.3E+13	4.0E+12	2.6E+12	2.3E+12
47	$H_9C_{11}^+ + C_2H_2 = C_{13}H_8H^+ + H_2$	-7.2	5.5E+14	5.5E+14	5.5E+14	2.8E+14
48	$H_9C_{11}^+ + C_2H_2 = C_{13}H_6H_3^+ + H_2$	-216.0	5.5E+14			
49	$C_{12}H_9^+ + C_2H_2 = C_{14}H_8H_3^+$	-6.1	5.5E+14			
50	$H_9C_{12}^+ + C_2H_2 = C_{14}H_8H_3^+$	-149.0	5.5E+14			
51	$C_{12}H_9^+ + C_4H_2 = C_{16}H_{11}^+$	-255.1	5.6E+14			
52	$H_9C_{12}^+ + C_4H_2 = C_{16}H_{11}^+$	-398.0	5.6E+14			
53	$H_9C_{12}^+ + C_4H_2 = C_{16}H_{10}H^+$	-135.8	5.6E+14			
54	$C_{13}H_8H^+ + M = C_{13}H_6H_3^+ + M$	-208.9	4.5E+14			
55	$C_{13}H_6H_3^+ + C_2H_2 = C_{15}H_{10}H^+$	14.2	5.4E+14			
56	$C_{13}H_8H^+ + C_2H_2 = C_{15}H_{10}H^+$	-194.7	5.4E+14			
57	$C_{13}H_8H^+ + C_4H_2 = H_{11}C_{17}^+$	-258.2	5.6E+14			
58	$C_{13}H_8H^+ + C_4H_2 = C_{17}H_{11}^+$	-130.7	5.6E+14			
59	$C_{13}H_6H_3^+ + C_4H_2 = C_{17}H_{11}^+$	78.1	5.6E+14			
60	$C_{13}H_6H_3^+ + C_4H_2 = H_{11}C_{17}^+$	-49.3	5.6E+14			
61	$C_{14}H_8H_3^+ + C_2H_2 = C_{16}H_{11}^+ + H_2$	-242.1	5.4E+14			

No.	REACTION	ΔS(1750)	Forward Rate Coefficient, k, $cm^3/mole/s$ 500	1000	1500	2000
62	$C_{14}H_8H_3^+ + C_2H_2 = C_{16}H_{10}H^+ + H_2$	20.0	4.0E+14	2.3E+14	2.2E+14	2.2E+14
63	$C_{15}H_{10}H^+ + C_2H_2 = C_{17}H_{11}^+ + H_2$	70.8	1.4E+14	1.5E+13	3.0E+12	6.1E+12
64	$C_{15}H_{10}H^+ + C_2H_2 = H_{11}C_{17}^+ + H_2$	-56.6	5.4E+14			
65	$C_{16}H_{11}^+ + C_2H_2 = C_{18}H_{10}H^+ + H_2$	124.8	5.4E+14	5.6E+13	6.2E+11	6.3E+10
66	$C_{16}H_{11}^+ + C_2H_2 = H_{11}C_{18}^+ + H_2$	112.2	2.7E+11	2.7E+11	3.4E+11	4.7E+11
67	$C_{16}H_{10}H^+ + C_2H_2 = H_{11}C_{18}^+ + H_2$	-149.9	5.4E+14			
68	$C_{16}H_{10}H^+ + C_2H_2 = C_{18}H_{10}H^+ + H_2$	-137.4	5.4E+14			
69	$C_{16}H_{11}^+ + C_4H_2 = H_{11}C_{20}^+ + H_2$	-24.4	5.4E+14	5.4E+14	5.4E+14	5.7E+14
70	$C_{17}H_{11}^+ + C_2H_2 = C_{19}H_{11}^+ + H_2$	-234.7	5.3E+14			
71	$H_{11}C_{17}^+ + C_2H_2 = C_{19}H_{11}^+ + H_2$	-107.3	5.3E+14			
72	$H_{11}C_{18}^+ + C_2H_2 = H_{11}C_{20}^+ + H_2$	-129.8	5.3E+14			
73	$C_{18}H_{10}H^+ + C_2H_2 = H_{11}C_{20}^+ + H_2$	-142.4	5.3E+14			
74	$H_{11}C_{18}^+ + C_2H_2 = C_{20}H_{11}^+ + H_2$	50.9	5.3E+14	5.3E+14	1.0E+14	9.3E+12
75	$C_{18}H_{10}H^+ + C_2H_2 = C_{20}H_{11}^+ + H_2$	36.3	2.7E+13	4.2E+13	5.8E+13	7.0E+13
76	$C_{19}H_{11}^+ + C_2H_2 = C_{21}H_{11}^+ + H_2$	-49.9	5.3E+14			
77	$C_{20}H_{11}^+ + C_2H_2 = C_{22}H_{13}^+$	-333.6	5.3E+14			
78	$H_{11}C_{20}^+ + C_2H_2 = C_{22}H_{13}^+$	-152.9	5.3E+14			
79	$C_{21}H_{11}^+ + C_2H_2 = C_{23}H_{13}^+$	18.3	5.3E+14			
80	$C_{21}H_{11}^+ + C_3H_4 = C_{22}H_{13}^+ + C_2H_2$	-224.4	5.5E+14			
81	$C_{22}H_{13}^+ + C_2H_2 = C_{24}H_{13}^+ + H_2$	-77.7	5.3E+14			
82	$C_{22}H_{13}^+ + C_4H_2 = C_{24}H_{13}^+ + C_2H_2$	-84.5	5.3E+14			

C. ION-ELECTRON RECOMBINATION REACTIONS[a]

No.	REACTION	A	n
1	$H_3O^+ + e \rightarrow H_2O + H$	1.3E+19	-0.5
2	$HCO^+ + e \rightarrow CO + H$	7.4E+18	-0.68
3	$CH_3^+ + e \rightarrow CH + H_2$	5.3E+18	-0.5
4	$C_2H_3^+ + e \rightarrow C_2H + H_2$	8.5E+18	-0.5
5	$C_3H_3^+ + e \rightarrow C_2H_2 + CH$	1.1E+19	-0.5
6	$H_3C_3^+ + e \rightarrow C_2H_2 + CH$	1.1E+19	-0.5
7	$C_4H_5^+ + e \rightarrow C_2H_2 + C_2H_3$	1.2E+19	-0.5
8	$C_5H_2H^+ + e \rightarrow C_2H + C_3H_2$	1.3E+19	-0.5
9	$H_5C_5^+ + e \rightarrow C_3H_3 + C_2H_2$	1.4E+19	-0.5
10	$C_6H_5^+ + e \rightarrow C_4H_4 + C_2H$	1.4E+19	-0.5
11	$C_7H_4H^+ + e \rightarrow C_4H_2 + C_3H_3$	1.5E+19	-0.5
12	$H_7C_7^+ + e \rightarrow C_6H_4 + CH_3$	1.5E+19	-0.5
13	$C_8H_7^+ + e \rightarrow C_6H_6 + C_2H$	1.6E+19	-0.5
14	$C_9H_7^+ + e \rightarrow C_8H_6 + CH$	1.7E+19	-0.5
15	$H_7C_9^+ + e \rightarrow C_8H_6 + CH$	1.7E+19	-0.5
16	$C_{10}H_9^+ + e \rightarrow C_{10}H_8 + H$	1.8E+19	-0.5

No.	REACTION			A	n
17	$H_5C_{10}^+ + e$	→	$C_8H_6 + C_2H_3$	1.8E+19	-0.5
18	$C_{11}H_8H^+ + e$	→	$C_{10}H_8 + CH$	1.9E+19	-0.5
19	$H_5C_{11}^+ + e$	→	$C_8H_6 + C_3H_3$	1.9E+19	-0.5
20	$C_{12}H_9^+ + e$	→	$C_{12}H_8 + H$	1.9E+19	-0.5
21	$H_5C_{12}^+ + e$	→	$C_{10}H_8 + C_2H$	1.9E+19	-0.5
22	$C_{13}H_6H_3^+ + e$	→	$C_{13}H_9$	2.0E+19	-0.5
23	$C_{13}H_8H^+ + e$	→	$C_{12}H_8 + CH$	2.0E+19	-0.5
24	$C_{14}H_8H_3^+ + e$	→	$C_{14}H_{10} + H$	2.1E+19	-0.5
25	$C_{15}H_{10}H^+ + e$	→	$C_{14}H_{10} + CH$	2.1E+19	-0.5
26	$C_{16}H_{11}^+ + e$	→	$C_{16}H_{10} + H$	2.2E+19	-0.5
27	$C_{16}H_{10}H^+ + e$	→	$C_{16}H_{10} + H$	2.2E+19	-0.5
28	$C_{17}H_{11}^+ + e$	→	$C_{15}H_{10} + CH$	2.2E+19	-0.5
29	$H_{11}C_{17}^+ + e$	→	$C_{17}H_{11}$	2.2E+19	-0.5
30	$H_{11}C_{18}^+ + e$	→	$C_{16}H_{10} + C_2H$	2.3E+19	-0.5
31	$C_{18}H_{10}H^+ + e$	→	$C_{18}H_{10} + H$	2.3E+19	-0.5
32	$C_{19}H_{11}^+ + e$	→	$C_{16}H_{10} + CH$	2.3E+19	-0.5
33	$C_{20}H_{11}^+ + e$	→	$C_{18}H_{10} + C_2H$	2.4E+19	-0.5
34	$H_{11}C_{20}^+ + e$	→	$C_{20}H_{11}$	2.4E+19	-0.5
35	$C_{21}H_{11}^+ + e$	→	$C_{18}H_{10} + C_3H$	2.4E+19	-0.5
36	$C_{22}H_{13}^+ + e$	→	$C_{22}H_{12} + H$	2.5E+19	-0.5
37	$C_{23}H_{13}^+ + e$	→	$C_{22}H_{12} + CH$	2.5E+19	-0.5
38	$C_{24}H_{13}^+ + e$	→	$C_{24}H_{12} + H$	2.5E+19	-0.5

a $C_3H_3^+$ = linear $C_3H_3^+$; $H_3C_3^+$ = cyclic $C_3H_3^+$; C_3H_4 = allene; H_4C_3 = propyne; $C_6H_5^+$ = linear $C_6H_5^+$; C_2H_3 = linear $C_2H_3^+$; $C_7H_7^+$ = benzyl; C_3H_2 = H-C=C-CH; CH^* = doublet delta state of CH radical; $C_xH_y^+$, $H_yC_x^+$, $C_xH_{(y-n)}H_n^+$, etc. represent different isomers of the same ion.

nonpolar species such as the neutral growth species in our ionic model, except for propyne, Eq. (1) reduces to the Langevin equation which does not have a temperature coefficient. We have used Eq. (1) to calculate, where necessary, ion-molecule reaction rate coefficients for our soot growth model.

Several theoretical analyses have had the objective of defining the temperature effect on ion-molecule reactions but these have all concentrated on the situation when the neutral reactant has a dipole moment.[17,18,21–24] In the Langevin theory,[25] which forms the basis for these analyses, the ion is treated as a point charge. This is certainly not true for many of the large ions; even when the charge is localized it would be shielded from the approaching reactant by the rest of the molecule. Intuitively the larger ions should have a smaller rate coefficient and a negative temperature coefficient; we plan to improve the theoretical basis in an extension of this program.

Equation (1) accounts only for the number of collisions (it does not include collision efficiency) and fits most room temperature experimental rate coefficient data. There is considerable evidence that the rate of ion-molecule reactions is directly dependent upon the exothermicity of the reaction, ΔH_r and we hope to use such correlations to estimate the collision efficiency for this set of reactions but have not yet devised a logical means.

One of the major problems in working with large ions is their identification; mass spectrometry gives mass only. The number of carbon and hydrogen atoms has been determined by the use of isotopes.[5] Thus for a given molecular formula there can be several isomeric structures. We thus include several isomers for some ions when their free energies of formation are close; we seek a rational means of reducing this to "one isomer" per ion, probably by weighting the thermodynamic quantities, ΔH_f and C_p appropriately and by mechanistic considerations.

The present set of ion-molecule reactions, chosen from a set of about 318 reactions, is presented in Table I.B and Fig. 2. We have chosen to write the reactions always toward increasing molecular size; thus the free energy of reaction becomes more positive as the temperature is increased. To avoid excessively fast reverse reactions, we limit the forward reaction rate coefficient so that the reverse reaction never exceeds the Langevin rate calculated by Eq. (1). Because the temperature coefficient cannot be represented by an Arrhenius expression, this has caused some difficulties with Frenklach's code. Brown incorporates the effect with a table of free energies as a function of temperature.

C. ION-ELECTRON RECOMBINATION

In choosing product channels for the large ion-electron dissociative recombination reactions, only molecules observed by Bockhorn et al.[26] have been considered as products. Reaction rate coefficients for ion-electron reactions are not strongly temperature dependent, but they do increase with the size of the ion.

The ions disappear by either ion-electron or positive ion-negative ion recombination reactions. Negative ion recombination rate coefficients are about one to two orders of magnitude slower than electron recombination rate coefficients. Further, negative ion concentrations which have been measured are about two orders of magnitude smaller than electron concentrations[27] but there are no good measurements of electron or negative ion concentrations in soot forming flames. There is, however, evidence for the presence of large negative ions in soot forming flames.[5,28,29] We neglect negative ions for the present; they should be included in the future. Their inclusion would decrease the number of by-product neutral species which Frenklach improperly uses to compare the free radical and ionic mechanisms. In one computer run we reduced the ion recombination rate coefficient for all reactions by two orders of magnitude and it made a significant change in the ion concentrations.

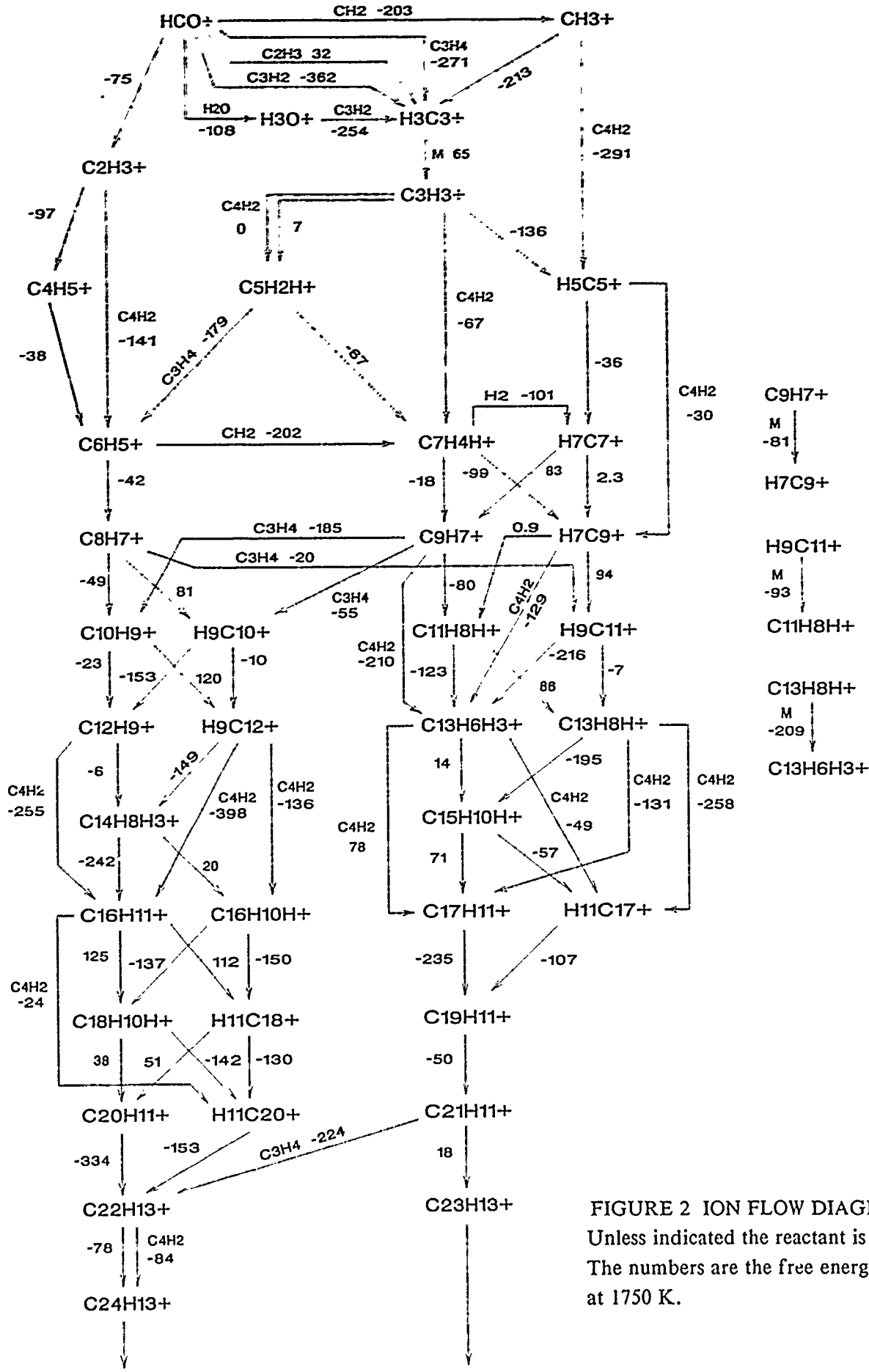

FIGURE 2 ION FLOW DIAGRAM
Unless indicated the reactant is C_2H_2.
The numbers are the free energy of react at 1750 K.

We estimate the rate of ion recombination, α, by the equation for the rate of collision of electrons with particles[30]

$$\alpha = \frac{\pi d^2}{4} \left[\frac{8kT}{\pi m_e}\right]^{1/2} \left[1 + \frac{e^2}{(2\pi\epsilon_0 d)kT}\right] \quad (2)$$

in which d = the ion diameter, m_e = the electron mass, and ϵ_0 = dielectric constant of free space. The ion diameters were calculated from ion mobilities by use of the Langevin equation for ion mobilities. Equation (2) gives a $T^{-1/2}$ temperature dependence which compares favorably with experiments of Ogram et al.[31] for H_3O^+. The values calculated by Eq. (2) were about twice the measured values of Ogram, so we have divided the calculated values by 2.

If there is an error in our recombination rates it will be on the high side. This is consistent with a comparison of experiment and computer runs. Generally, in the computer runs to date, most large ions (there are exceptions) are computed to have far too small a concentration and a more rapid decay rate than observed perimentally, see below. The small calculated concentration may be due to the ion-molecule rates being too small, or due to too fast a loss rate by ion-electron recombination. This could indicate the presence of significant concentrations of negative ions; their rates of recombination are smaller than for electrons. Of course, the recombination of a large positive ion and a large negative ion would double the size of the carbon species, albeit neutral, and could be interpreted as the first step in coagulation. Such collisions are favored, by electric charge effects, over ion-neutral or neutral-neutral collisions.

V. DIFFUSION

Because the pressure for the standard flame is less than one atmosphere and we have experimentally demonstrated the importance of diffusion[5] in the flame chosen for study, it is necessary to include the diffusion coefficients for ions. We estimated these using the procedure previously developed for interpreting Langmuir probe data.[7] Experimental ion mobilities of a wide mass range of PCAH ions[32,33] were extrapolated to the higher mass range required for this program. This extrapolation gives results of μ vs. ionic mass, amu, which parallels the results obtained from a calculation using the Langevin type equation, giving confidence in the procedure.

We assume that the negative species is a free electron, although there is some evidence that there are large negative ions present.[6,28] With electrons present the ambipolar diffusion coefficient of the ion must be used because the ions do not diffuse independent of electrons. The ambipolar diffusion coefficient (D_a) for a specific ion was calculated from the ion mobility using the relationship[34]: $D_a = 2kT\mu/e$, where k is Boltzmann's constant, T is temperature, μ is the ion mobility, and e is the elementary charge. The ionic mobility is calculated by the following procedure:

(1) Calculate the ion mobility, μ, at 2.67 kPa and 273 K for each of the dominant flame gases using the following correlations developed at AeroChem based on the Langevin equation combined with experimental values:

$$\mu_{i,j}(P_0, T_0) = a(j) \times (MW_i)^{b(j)} \text{ cm}^2 \text{ V}^{-1} \text{ s}^{-1} \quad (3)$$

where i is the ion species of mass MW_i and where a(j) and b(j), for each flame gas, j, are given in the following table: r^2 is the coefficient of determination of the fit to the actual data:

Gas	a	b	r^2
H_2	3471.53	-0.49893	0.9981
O_2	742.83	-0.48710	0.9981
CO_2	493.44	-0.46446	0.9975
C_2H_2	473.39	-0.43385	0.9991
CO	688.39	-0.47242	0.9989
H_2O	760.55	-0.46498	0.9984

(2) Correct each of the low pressure, low temperature ion mobilities calculated above, to flame pressures and temperatures, by the following formula (except for water), where P is the flame pressure (kPa) and T is temperature of the flame:

$$\mu_{i,j}(P, T) = \frac{P_0}{P} \times \left[\frac{T}{T_0}\right]^{0.72} \times \mu_{i,j}(P_0, T_0) \tag{4}$$

For water vapor:

$$\mu_{i,H_2O}(P, T) = \frac{P_0}{P} \times \left[\frac{T}{T_0}\right]^{1.16} \times \mu_{i,H_2O}(P_0, T_0) \tag{5}$$

(3) Correct the ion mobility calculated for each of the pure gases, and evaluated at flame conditions, to the actual flame gas composition using Blanc's Law - i.e., a simple viscosity mixing rule;

$$\mu_i^{-1} \text{ (for the gas mixture)} = \sum_j \frac{X_j}{\mu_{i,j}} \tag{6}$$

where X_j is the mole fraction of gas j in the flame, and μ_i is the overall ion mobility of the ith ion in the gas mixture.

It was apparently difficult to incorporate this into Frenklach's computer program so that he has employed a different procedure for including the diffusion coefficient.[4]

VI. COMPARISON OF CALCULATED AND EXPERIMENTAL ION CONCENTRATION PROFILES

Frenklach and Wang[4] have run a limited number of computer runs using the sets of reactions we developed for the ionic mechanism of soot formation. The early runs showed great differences between experimental and computed ion profiles. As the model was improved the agreement

improved. There were no arbitrary alterations of rate constants or of thermodynamics. The major changes were in the choice of reactions and in the isomer used; large ions have a large number of isomers, so this gives a large range of choices. Without making such choices the number of reactions and reactants becomes excessive for the computer memory. The effect of such choices on the realism of models has yet to be evaluated.

Some selected comparisons between calculated and experimental ion profiles are presented in Figs. 3 and 4. For small ions, Fig. 3, the agreement is reasonably good. The relationship of the two isomers $H_3C_3^+$ and $C_3H_3^+$, the cyclic and linear isomers of the proposed precursor ion, demonstrates that equilibrium maintains a relatively high concentration of the reactive isomer. One of the arguments against the ionic mechanism was that the stable isomer $H_3C_3^+$ was found experimentally to be nonreactive with acetylene or other small hydrocarbons[35,36] and thus because of this ion's stability ionic growth would not proceed. The linear isomer was found to be very reactive.[35,36]

The data for larger ions, Fig. 4, are not in such good agreement. The peak concentrations are reasonably close but the profiles differ markedly. This difference is, however, no greater than the difference for neutral species in the free radical mechanism, where it is declared as good agreement. One major difference between our approach to modeling and Frenklach's is that we have limited the reactants and products to those that have been observed experimentally and have required that the model calculate all such species. Frenklach's model does not have either of these constraints.[4] Thus his model includes cyclopentaphenanthrene which is not observed experimentally, and does not include phenanthrene and pyrene which are observed experimentally. Further, in Frenklach's model,[4] only five calculated cyclic compound profiles are compared with experiment and the peak concentration of one of these, naphthalene, is computed to be 20 times smaller than measured.

The calculated ion concentrations increase with distance and the experimental concentrations decrease, Fig. 4. A calculation was carried out in which the temperature was fixed at the maximum temperature (the temperature profile is an input parameter); the calculated concentrations then decayed slowly. This shows the sensitivity to temperature. In an early computer experiment a point was misplaced in the temperature rise section of the temperature profile and this produced a corresponding change in the ion profile, confirming the temperature sensitivity of the computer model.

We compare, in Fig. 5, the maximum concentration of ions experimentally observed and calculated. Since the experiments do not distinguish between isomers and sometimes there are more than one isomer in the computer program, we compare in Fig. 5 the isomer in which the agreement is best between the calculated and experimental concentrations. For most of the larger ions, the experimental value exceeds the calculated value. We have neglected electron attachment and thus positive ion-negative ion recombination, which if included would increase the calculated concentrations; ions would not be removed from the system as fast as by ion-electron recombination. Incidentally this would decrease the formation of neutral species which Frenklach incorrectly interprets as a measure of the efficacy of the ion-molecule mechanism.

The free radical mechanism which is used to produce the precursor ion in the computer model does not agree well with experimental measurements of these neutral species, Fig. 6. The experimental measurements have been made by several people with good agreement. The question is thus raised: does the difference between experiment and calculation for the ionic mechanism depend upon the problems in the free radical mechanism or are they problems in the ionic mechanism? This could be readily tested if the experimental neutral species profiles required for the ionic mechanism could be an input to the computer program, just as the temperature is. Frenklach could not handle this with his program so the test was done by Brown and Pedersen whose computer program does have this capability. First they ran the program using as input the calculated neutral species concentrations from Frenklach. The resulting ion profiles were very close to those calculated

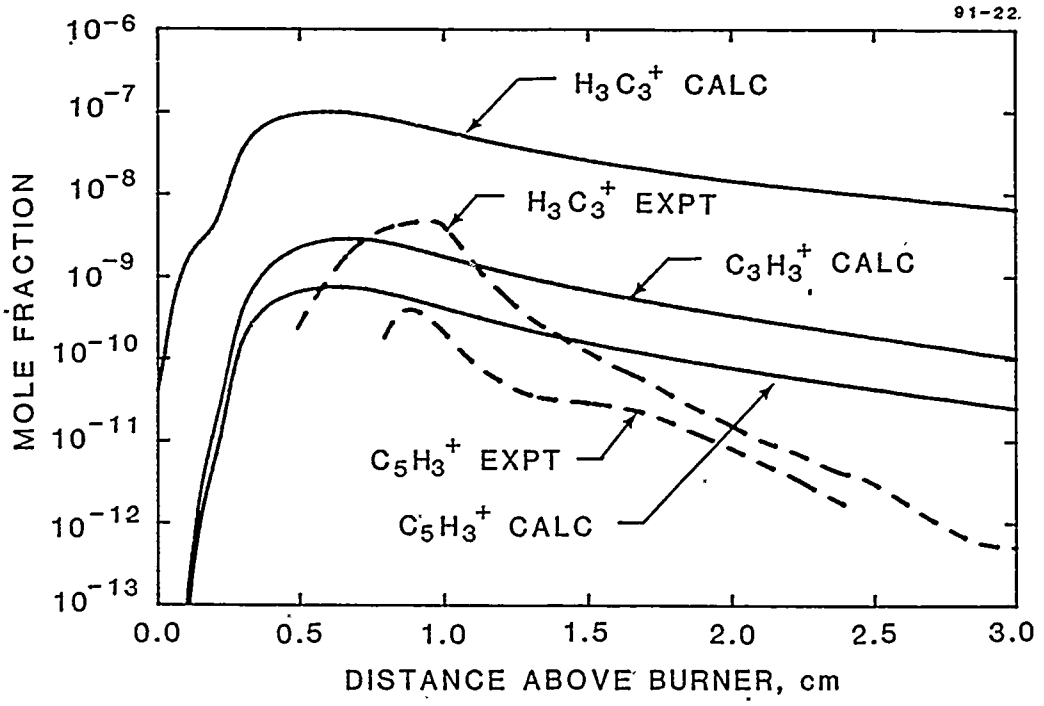

FIGURE 3 COMPARISON OF EXPERIMENTAL AND CALCULATED $C_3H_3^+$ AND $C_5H_3^+$ CONCENTRATION PROFILES

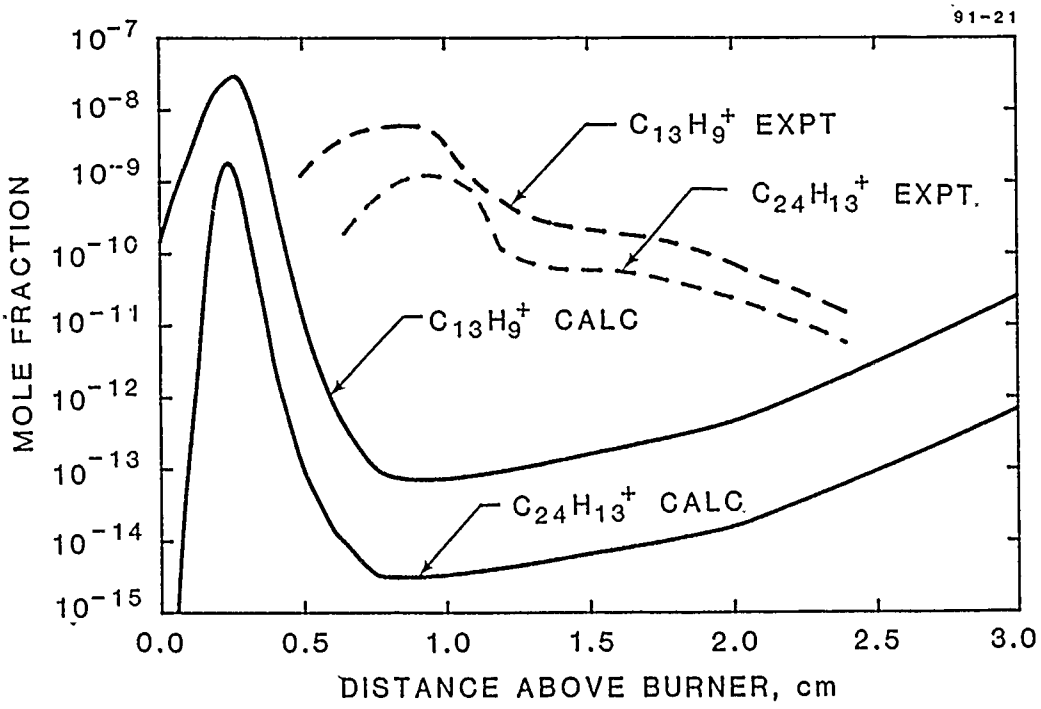

FIGURE 4 COMPARISON OF EXPERIMENTAL AND CALCULATED $C_{13}H_9^+$ AND $C_{24}H_{13}^+$ ION PROFILES

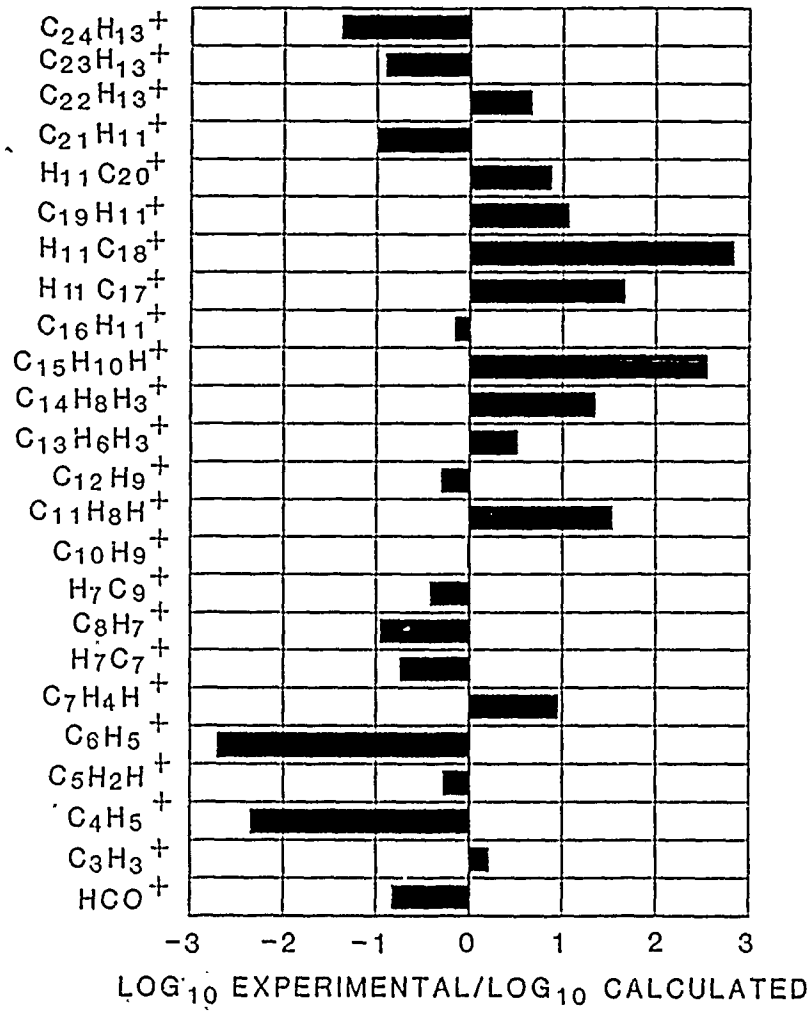

FIGURE 5 COMPARISON OF PEAK EXPERIMENTAL AND CALCULATED ION CONCENTRATIONS

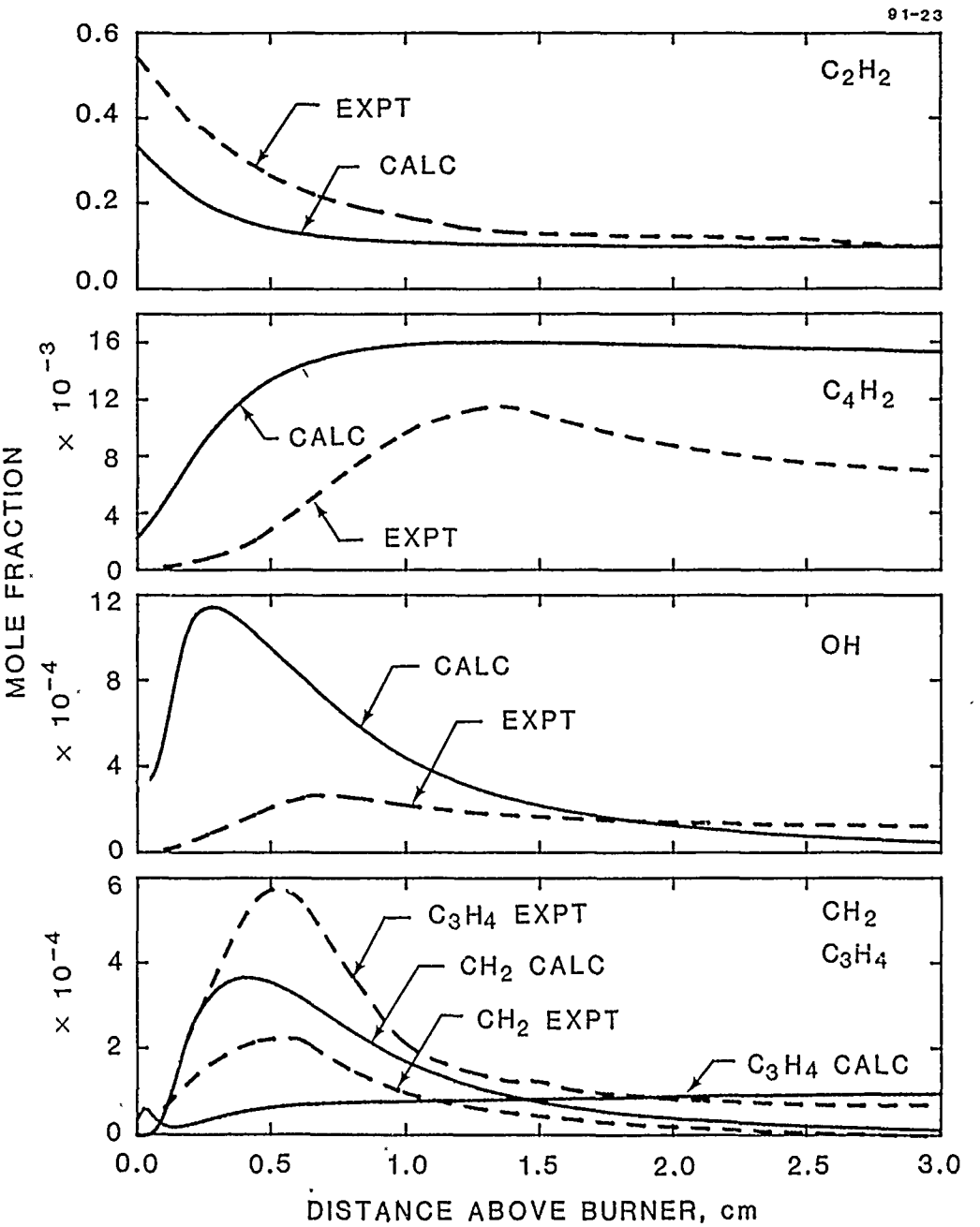

FIGURE 6 COMPARISON OF EXPERIMENTAL AND CALCULATED NEUTRAL SPECIES CONCENTRATIONS

by Frenklach, confirming the validity of the technique of using concentration profiles as input to the computer program.

When Brown and Pedersen then ran the program using as input the experimental neutral species profiles required by the ionic mechanism, the maximum calculated ion concentrations were many orders of magnitude lower than measured! This indicates a great sensitivity in the computer model to the free radical mechanism. One has to ask the question: how meaningful are such models if they are so sensitive? This question has yet to be answered; more sensitivity analyses are clearly called for and will be done in the extension of the present work. The only real way to test a model is to apply it to more than one system. We also plan to do this in the extension of this work when we will apply this model to the benzene flame.

VII. COMPARISON OF THE RATE OF CARBON SPECIES GROWTH FOR THE FREE RADICAL AND IONIC MECHANISMS

A simple technique has been employed to compare the relative rates by which the two competing mechanisms account for the growth of carbon containing species in the same sooting flame. It is accepted that soot is formed from small carbonaceous molecules by a mechanism in which they increase in size and carbon to hydrogen ratio until at some size they coagulate to produce even larger species, and eventually produce incipient soot particles. The least understood steps in this process are the increase in carbon number from two to a molecular weight of about 1,000 u. In this comparison we use experimental data combined with reaction rate coefficients to compare the rates, and thus times, for the addition of ten carbon atoms to the growing molecular species in the range of carbon numbers for which experimental data are available. The range of observed carbon numbers is very limited for neutral species because as they become larger their concentration rapidly diminishes below detectability.

For this comparison we chose the well studied acetylene/oxygen flat flame at 2.67 kPa, equivalence ratio = 3.0 and unburned gas velocity = 50 cm/s. For the experimental neutral species concentrations we use those of Vovelle[3] because they extend to mass 252 u. Bittner and Howard's data[8] extend only to mass 178, $C_{14}H_{10}$, and at mass 178 are more than an order of magnitude less than those of Vovelle. This choice favors the free radical mechanism. For the free radical mechanism, free radical concentrations have not been measured, so they are assumed equal to the concentration of the preceding neutral species from which the radical was formed. This again favors the free radical mechanism.

For the individual ionic species concentrations, we use those measured at AeroChem[5]; the total concentrations have been confirmed by Gerhardt and Homann[29] and are consistent with measurements of Delfau, Michaud and Barassin.[37]

For the free radical mechanism we use that of Frenklach and Warnatz[38] and use the rate coefficients of Frenklach and Wang[39] for the specific steps. The free radical mechanism involves four elementary reactions with the following rate coefficients:

R is the large reactant species.

$R + H\bullet\ (-H_2)$	$k = 4.5 \times 10^{12}\ cm^3\ mol^{-1}\ s^{-1}$
$R + C_2H_2\ (-H\bullet)$	$k = 3.1 \times 10^{12}$
$R + C_2H_2$	$k = 1.0 \times 10^{13}$
$R + H\bullet$	$k = 1.3 \times 10^{13}$

The ionic mechanism for growth requires two reactions:

$$R^+ + C_2H_2\,(-H_2) \qquad k = 3.6 - 5.3 \times 10^{14}$$
$$R^+ + C_2H_2 \qquad k = 5.6 \times 10^{14}$$

The ion–molecule reaction rate coefficients are calculated by Langevin theory for each reaction and are adjusted so that the reverse reaction rate calculated by thermodynamic equilibrium never exceeds the Langevin rate calculated for the reverse reaction.

The times for the species to add a specified number of carbon atoms by the two mechanisms were then compared. Thus, for the reaction:

$$A + B \rightarrow C + D$$

the rate of reaction is given by:

$$R = \frac{dC}{dt} = kAB \tag{7}$$

For this analysis we use the maximum (with respect to distance from the burner) experimental concentrations of A, and use the measured value of B at the position in the flame where the concentration of A is maximum. The appropriate rate coefficient for k is used for either the free radical or the ionic mechanism. In the free radical mechanism,[38,40] A is a stable species or a free radical and C is a free radical with the same number of carbon atoms as A, or a stable species with two more carbon atoms than A; B is a hydrogen atom or acetylene. In the ionic mechanism, A is an ion and C is an ion with two more carbon atoms than A; B is acetylene.

The reaction time is calculated from the experimental maximum concentration of the growing species, the concentration of the smaller reactant, H•, H_2, or C_2H_2, at the distance in the flame at which the growing species maximizes and the reaction rate coefficient, by:

$$\tau = n/R \tag{8}$$

where n is the number of reacting species flowing through the system, i.e., 4×10^{14} cm^{-3}; and R is the reaction rate for any step.

The times required for 4×10^{14} cm^{-3} growing neutral or ionic species to add ten carbon atoms are displayed in Fig. 7 for each step in the mechanism and for the total time. The time for the reverse reaction for each step is also given. The reverse time is the rate of the reverse reaction calculated from thermodynamic equilibrium. The number density of reactive species of any given variety, 4×10^{14} cm^{-3}, is chosen because this is the maximum number of soot particles observed in this flame.

The total times to add ten carbon atoms by the two mechanisms are comparable: 8.1 μs for the free radical mechanism and 6.7 μs for the ionic mechanism.

These total times do not include reverse reactions which should be taken into account; a rapid reverse reaction, small time, can effectively reduce the forward rate of reaction, depending on the rates and equilibria of the preceding and following reaction steps. The reverse reactions, given in Fig. 7, appear to be a greater complication in the free radical mechanism than in the ionic mechanism. An indication of the forward reaction rate reduction is given by the ratio of forward to reverse reaction times; when this value exceeds 1, the reaction proceeds more rapidly in the reverse reaction than in the forward direction; of course, the overall effect is more important when the forward reaction time for any individual step is long compared to the average reaction time.

FREE RADICAL MECHANISM

		Time, μs Forward	Reverse
$C_{10}H_8$			
‖	+ H • (- H_2)	0.26	0.12
$C_{10}H_7$•			
‖	+ C_2H_2 (- H•)	0.02	0.02
$C_{12}H_8$			
‖	+ H • (- H_2)	0.44	0.05
$C_{12}H_7$•			
‖	+ C_2H_2	0.01	2×10^{-6}
$C_{14}H_9$			
‖	+ C_2H_2 (- H)	0.07	0.06
$C_{16}H_{10}$•			
‖	+ H• (-H_2)	1.9	0.02
$C_{16}H_9$•			
‖	cyclizes		

		Time, μs Forward	Reverse
$C_{16}H_9$•			
‖	+ C_2H_2 (- H•)	0.12	0.11
$C_{18}H_{10}$			
‖	+ H• (- H_2)	3.2	0.35
$C_{18}H_9$•			
‖	+ C_2H_2	0.1	1×10^{-5}
$C_{20}H_{11}$			
‖	+ H•	2.1	55
$C_{20}H_{12}$			

Total Time = 8.1 μs

IONIC MECHANISM

		Time, μs Forward	Reverse
$C_{11}H_9^+$			
|	+ C_2H_2 (-H_2)	3.6	3×10^4
$C_{13}H_9^+$			
‖	+ C_2H_2	0.51	8×10^{-6}
$C_{15}H_{11}^+$			
|	+ C_2H_2 (- H_2)	0.64	3×10^4
$C_{17}H_{11}^+$			
|	+ C_2H_2 (- H_2)	1.3	3×10^5
$C_{19}H_{11}^+$			
‖	+ C_2H_2 (- H_2)	0.65	20
$C_{21}H_{11}^+$			

Total Time = 6.7 μs

FIGURE 7 TIMES TO ADD TEN CARBON ATOMS

The above analysis does not permit a clear decision between the free radical mechanism and the ionic mechanism. For modest size carbon species, 10 to 20 carbon atoms, the rate of growth of carbon species is about the same for the free radical mechanism and for the ionic mechanism. The greater concentration of neutral species is balanced by the greater reaction rate coefficients for ion-molecule reactions and the fewer number of steps involved in adding a specific number of carbon atoms to the growing species for the ionic mechanism, five steps, than for the free radical mechanism, eleven steps. The free radical mechanism suffers in the comparison because of lack of experimental data for the free radicals involved and for larger molecular species. The free radical mechanism also appears to have greater complications than the ionic mechanism due to reverse or equilibrium reactions.

Consider the implications of the above calculation of reaction times to determine the reasonableness of this approach. The maximum soot number density, Fig. 2 in Ref. 9, is reached at about 35 mm above the burner, or about 6.7 ms from the position in the flame at which large carbon containing species maximize. This is a good estimate of the time available, τ_s, for soot particles to be formed from molecular species. If we assume the time for the addition of one carbon atom to the growing species is τ_c, then the number of carbon atoms, N_c, that can be added to the growing nuclei is:

$$N_c = \frac{\tau_s}{\tau_c} = \frac{6.7 \times 10^{-3}}{7.4 \times 10^{-7}} \approx 9{,}000 \text{ carbon atoms.} \qquad (9)$$

τ_c is taken as the average for the neutral and ion mechanisms. 9,000 carbon atoms corresponds to a molecular weight of about 110,000 u, equivalent to a particle diameter of about 4.5 or 3.0 nm, depending upon whether the particle is planar or spherical, respectively.[41] The experimentally observed particle diameters at 35 mm above the burner surface are 9–13 nm for neutral particles and 3–6 nm for charged particles. It is interesting that the calculated diameter, assuming the equivalent of a fixed rate (fixed time) for adding carbon atoms to the growing species, neutral or ion, leads to a diameter of the carbon particle very close to that observed, within the accuracy of the calculation and the measurement.

The above discussion demonstrates that examining relative growth of small carbon species does not permit a conclusion concerning the rate of soot nucleation by the free radical and the ionic mechanism; they each have about the same reaction times using the available data. To make a distinction between the two mechanisms one must examine reactions involving larger numbers of carbon atoms.

Note the decrease in maximum concentration in going from C_6H_6 to $C_{14}H_8$ in the standard flame:

benzene	C_6H_6	7.8×10^{12} per cm^{-3}
naphthalene	$C_{10}H_8$	1.8×10^{11}
ethynylnaphthalene	$C_{12}H_8$	6.9×10^{10}
	$C_{14}H_8$	1.7×10^{10}

This is a decrease in concentration of about a factor of 60 per carbon atom added. Bockhorn's results,[26] which cover a larger range of carbon species do not indicate such a rapid decay, but unfortunately they are in a different flame.

For ions, the decay in concentration is much less,[5] e.g.:

$C_3H_3^+$	4.7×10^8 per cm^{-3}
$C_{30}H_{15}^+$	1.9×10^7
$C_{45}H_{17}^+$	1.9×10^6

This is a decrease in concentration of about a factor of 6 per carbon atom added, about one-tenth that indicated above for free radical species!

Clearly a comparison of the two mechanisms requires extension to much larger species than is done here. The computer modeling effort will thus have to be extended to greater masses than are currently in the computer model.

VIII. EXPERIMENTAL RATES OF ION FORMATION

One requirement of any mechanism of soot formation is that the rate of formation of soot precursors equal or exceed the rate at which soot is produced. In this section we examine previously obtained[5] experimental data for the total ions and the individual ions.

First we examine the experimental data presented in Fig. 8 to compare the experimental rate at which the total number of ions is generated with the rate at which neutral soot is observed to be formed. The temperature, total ion concentration, and the neutral and charged soot particle concentration profiles are presented in Fig. 8. Identifiable soot particles, (i.e those which can be detected using an electron microscope, diameter exceeding about 1.5 nm) first appear at about 2.0 cm above the burner, yet a yellow glow, presumably due to soot, first appears at about 1.0 cm. To reflect this observation, i.e., that soot is formed where the yellow glow appears even though the particles are too small to be detected with the electron microscope,,we have drawn, in Fig. 8, an interpolated (dotted) soot concentration curve starting at 1 cm and extending to the measured maximum.

We treat the flame as a steady state, one-dimensional system. The continuity equation describing the ion concentration at any distance from the burner is:

$$(dI/dt) = (\text{net ion production rate}) - V(dI/dx) + D(d^2I/dx^2) = 0 \qquad (10)$$

where I = ion concentration, V = flow velocity, D = ion diffusion coefficient, and x is the distance from the burner. V has been determined as a function of distance in this flame[6] and D was calculated from estimated ion mobilities, μ,[6] using the Einstein relation: $D = \mu(kT/e)$, where k is the Boltzmann constant and e the electronic charge. Combining these values with the ion concentration derivatives of the profile in Fig. 8 gives the "net ion production rate" as shown in Fig. 9.

The total ion production rate, q, was obtained by adding the calculated ion loss rate by recombination with free electrons, to the "net ion production rate". The ion recombination rate is αI^2, where α is the ion-electron recombination coefficient. For α we used 2×10^{-7} cm^3 s^{-1} where small (i.e., 39 amu) ions dominate, and corrected for increasing ion mass downstream in the flame[6] using a factor proportional to d^2 where d = ion diameter and a capacitive term of the form $(1 + A/d)$ with A a constant. The total ion production rate, q, is also plotted in Fig. 9 as a dashed line--note scale change. If negative ions are assumed to be the recombining partners for positive ions, the total ion production rates would be reduced because ion-ion recombination is slower by almost an order of magnitude than ion-electron recombination.

The net ion production rate shows two peaks corresponding to the two peaks in the ion concentration curve, the source of these two peaks is unknown. Also shown in Fig. 9 is the net rate

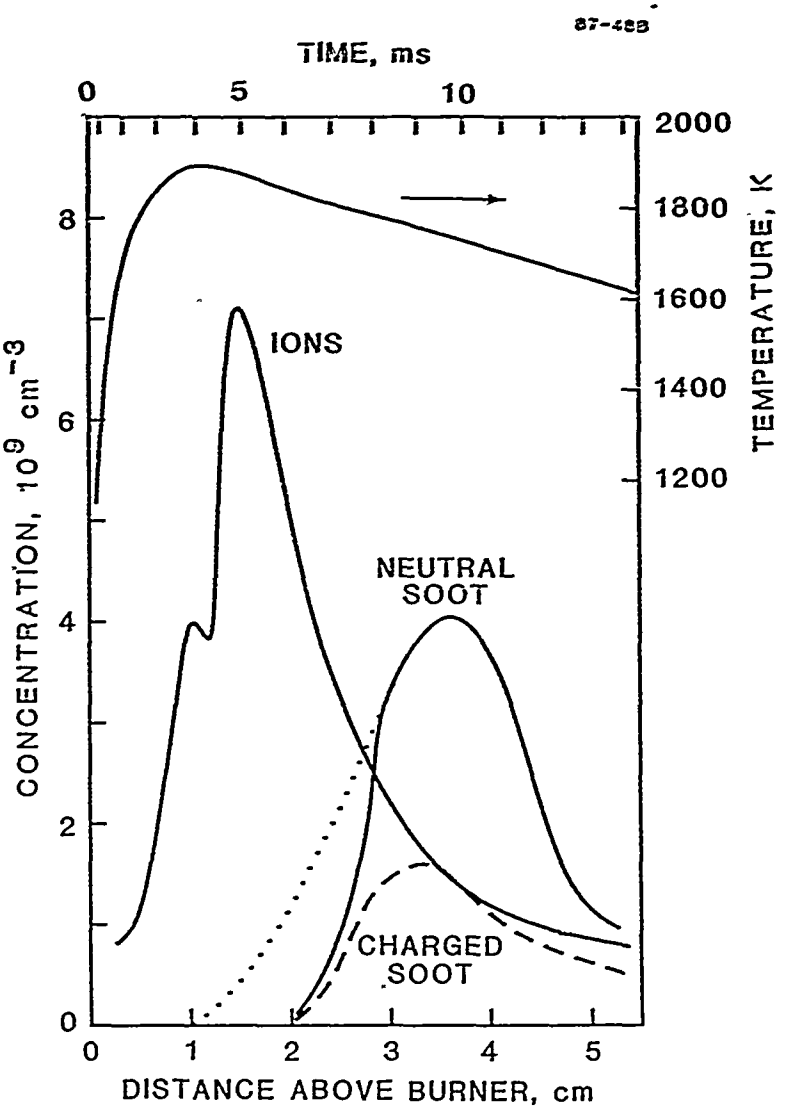

FIGURE 8 COMPARISON OF TOTAL ION CONCENTRATION AND SOOT CONCENTRATION PROFILES

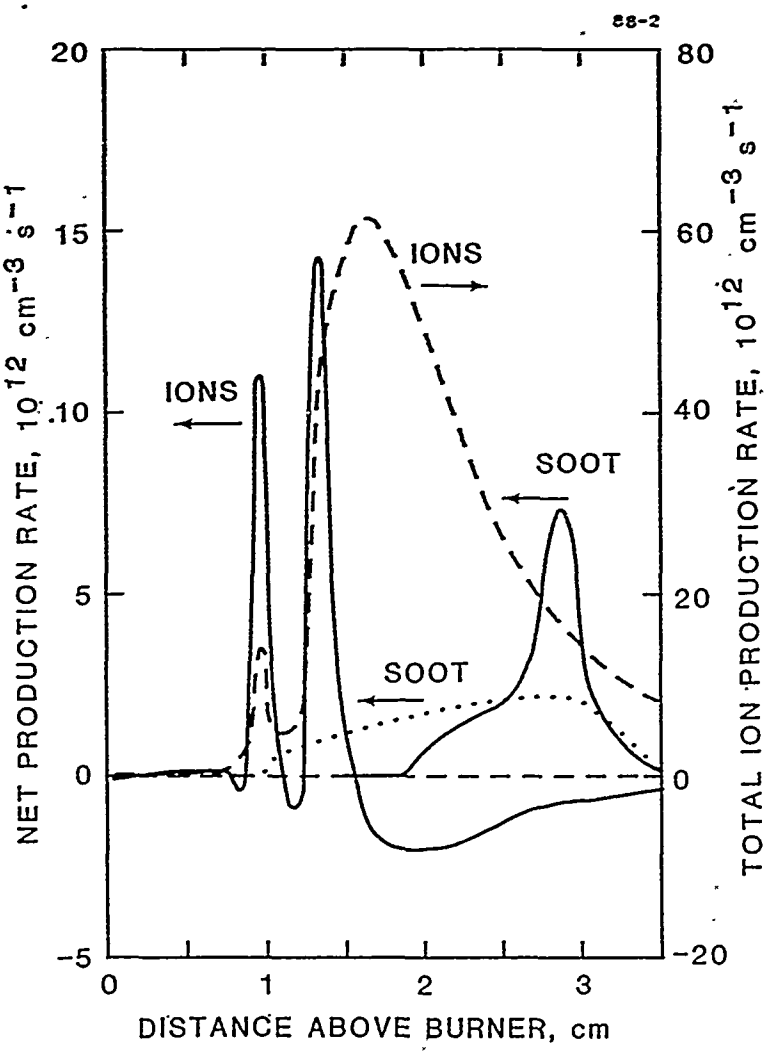

FIGURE 9 EXPERIMENTAL PRODUCTION RATES OF TOTAL IONS AND SOOT FORMATION

of particle formation derived from the two neutral soot curves in Fig. 8 using Eq. (10), in which the diffusion term for these large particles is now negligible compared with the flow velocity term.

The first observation is that the maximum net rate of ion formation, 1.5×10^{13} ions cm^{-3} s^{-1}, exceeds the net rates of soot formation, 2.5 and 7.5×10^{12} particles cm^{-3} s^{-1} from either curve. Second, the net ion loss and soot formation occur in the same region of the flame. Third, the net ion loss rate, about 2×10^{12} cm^{-3} s^{-1}, corresponds with the net particle formation rate, about 2×10^{12} cm^{-3} s^{-1} assuming particles first appear at the position in the flame where yellow first occurs (dotted curve, Figs. 8 and 9). The peak particle production rate for the measured soot curve is only about four times greater than the peak ion net loss rate. The value for the net ion disappearance rate, however, does not include larger ions lost by recombination which can still lead to soot formation via the same types of reactions as in the postulated free radical mechanisms, see Fig. 1.

These analyses lend further support to an ionic mechanism of soot formation in this flame. Clearly more precise data are desirable, particularly on negative molecular ions and on their rates of recombination, and particle concentration and particle size distribution (both neutral and charged) where soot is first observed, i.e., where the yellow emission first appears.

The experimental rates of formation and destruction for three ions, $C_3H_3^+$, $C_{13}H_9^+$, and $C_{21}H_{11}^+$ are shown in Figs. 10–12. In all three examples, the maximum rates of formation and destruction are the order of 10^{12} ions cm^{-3} s^{-1}, consistent, within the experimental accuracy, with the rate of soot formation. Further, these small ions start to disappear almost exactly at 1.0 cm where soot is first observed in this flame. These observations are again consistent with the ionic mechanism of soot formation. A similar comparison cannot be made for the free radical mechanism because measurements are not available.

IX. RECOMMENDATIONS FOR FUTURE WORK

Future work on soot formation should be concentrated on solving problems as opposed to producing more measurements. Computer modeling is the basis for interpreting the mechanism, from nucleation to final agglomeration; experimental work should be driven by the need of modelers. Understanding the nucleation step remains the major challenge, all of the other steps in the process are reasonably well understood.

The major experimental need for the free radical mechanism is for information on profiles of species larger than mass 252 u, five aromatic rings. This is the largest neutral species profile available in a sooting flame to compare with models. If, as appears to be the case, the experimental measurements are unavailable because the concentrations become too small to measure when the size exceeds 252, then there is reason to question the validity of the free radical mechanism. Reaction rates, for such small concentrations, would be too small to produce soot at the observed rates of production. This is not an easy measurement to make. It will have to be done with a molecular beam sampling mass spectrometer which uses photoionization. Commonly used thermal electron fragmentation of the parent species makes it difficult to identify the parent species. Both stable and free radical species must be measured.

Mass spectrometry is an intrusive technique and has thus been neglected, the major effort has been on nonintrusive techniques. Expensive and time intensive laser techniques have not been capable of identifying and quantifying the PCAH species in sooting flames. The spectra obtained are too diffuse to allow this type of analysis. It is now time to use the best available experimental techniques to obtain the required data.

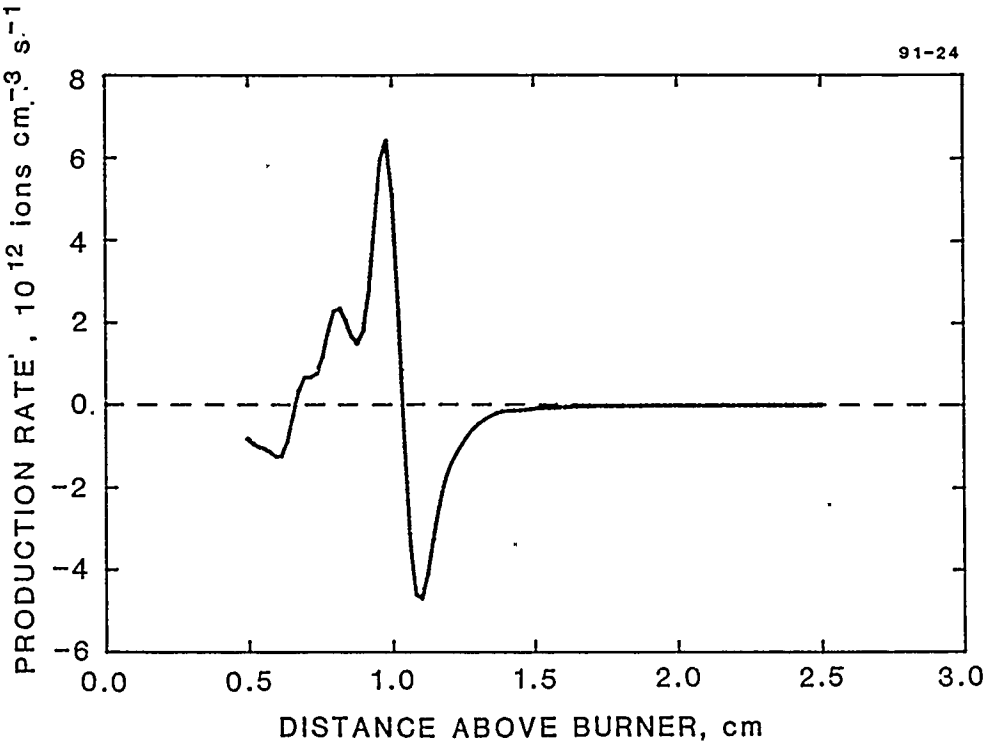

FIGURE 10 NET EXPERIMENTAL PRODUCTION RATE OF $C_3H_3^+$

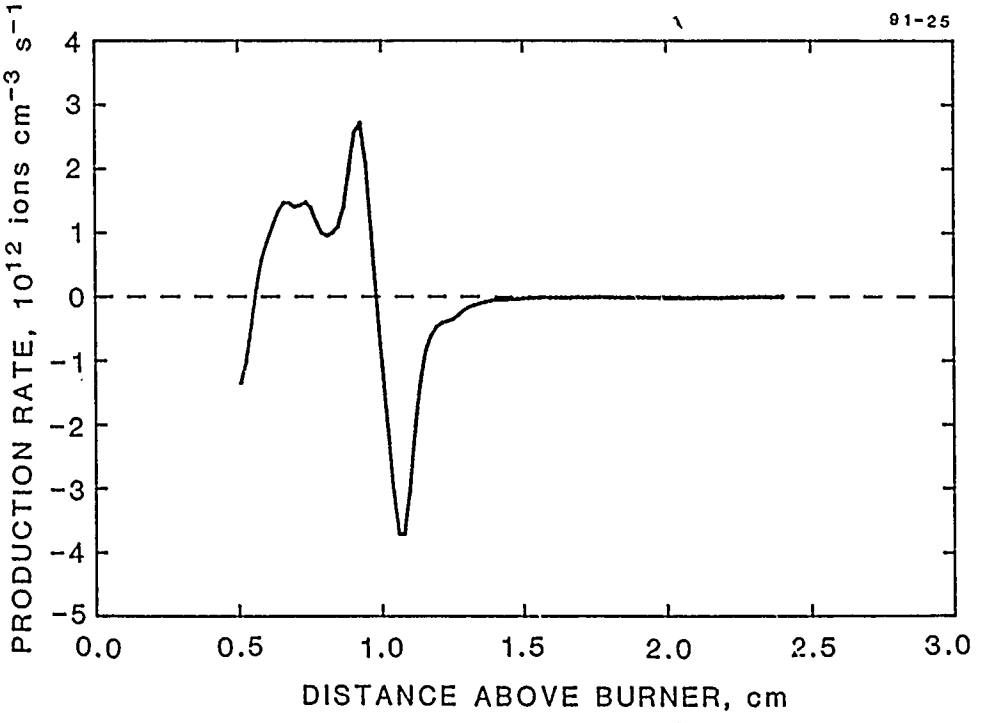

FIGURE 11 NET EXPERIMENTAL PRODUCTION RATE OF $C_{13}H_9^+$

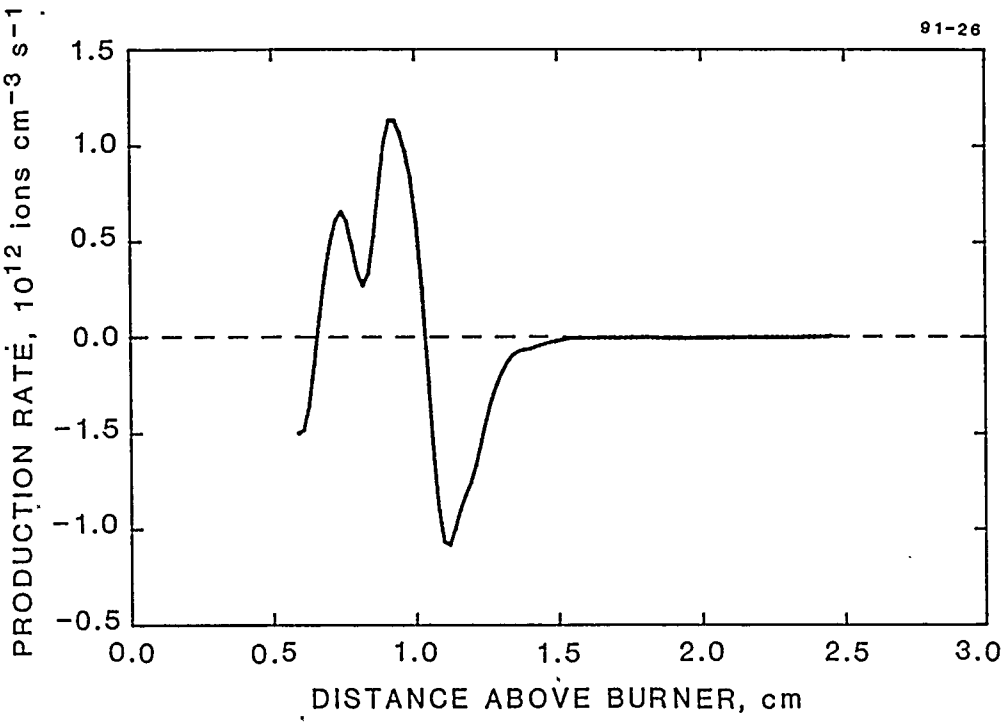

FIGURE 12 NET EXPERIMENTAL PRODUCTION RATE OF $C_{21}H_{11}^+$

Another major experimental need which is not being addressed is the rate at which incipient soot particles are formed. The concentration profiles of species falling between large ions (and large neutral species) and small soot particles are needed. This is also difficult to measure. The data are however very important for understanding both the free radical and the ionic mechanisms.

The major experimental need for the ionic mechanism is concentration profiles of negative ions in both the standard acetylene flame and in the benzene flame in which Howard and associates have measured neutral species profiles and AeroChem has measured positive ion species profiles.

For all experimental work, it is extremely important that a variety of measurements be made on the same flame by a number of researchers to reduce the degree of freedom which modelers currently enjoy because of limited data on any given system. Unless a flame is well documented, which no one research group can do, experimental measurements are essentially worthless. A few experimental measurements on a unique flame can be used to prove most anything and can very easily be simulated by models. The conclusions are worthless. Unfortunately the literature is replete with such measurements and interpretations.

X. PUBLICATIONS

1. Calcote, H.F. and Keil, D.G., "The Role of Ions in Soot Formation", Pure & Appl. Chem. 62, 815 (1990).

2. Gill,.R.J. and Calcote, H.F., "Thermodynamic Properties of Organic Cations", to be submitted to J. Chem. Thermodyn.

3. Calcote, H.F. and Gill, R.J., "A Detailed Mechanism of Ion Growth Related to Soot Formation in Flames" to be submitted to Combust. Flame.

4. Calcote, H.F. and Gill, R.J., "A Comparison of the Rate of Carbon Addition by the Ionic and Free Radical Mechanisms of Soot Formation in Flames," to be submitted to Combust. Flame.

5. Wang, H., Gill, R.J., Frenklach, M., and Calcote, H.F., "Computer Model Comparison of the Rate of Soot Production by the Neutral and Ionic Mechanisms of Soot Formation in Flames," to be published in Combust. Flame.

We list publications from a previous AFOSR program (Contract F49620-83-C-0150) which were published during this report period, these set the background for the present work:

1. Calcote, H.F., Olson, D.B., and Keil, D.G., "Are Ions Important in Soot Formation?" Energy & Fuels 2, 494 (1988).

2. Calcote, H.F. and Keil, D.G., "Ion-Molecule Reactions in Sooting Acetylene-Oxygen Flames," Combust. Flame 74, 131 (1988).

XI. PROFESSIONAL PARTICIPATION

The Principal Investigator on the program was H. F. Calcote who has been responsible for developing the reaction mechanism and collecting the reaction kinetics data. Dr. R.J. Gill has been responsible for collecting and calculating the thermodynamics data. We both acknowledge fruitful discussions with Drs. W. Felder and D. G. Keil.

XII. TECHNICAL INTERACTIONS

1. Poster: "An Ionic Mechanism of Carbon Formation in Flames," at NASA Symposium "Carbon in the Galaxy," Ames Laboratory, CA, 5, 6 November 1987.

2. Presentation: "Soot Formation in Flames," at NASA Lewis on 22 September, 1988.

3. Presentation: "The Role of Ions in Soot and Diamond Formation," at Symposium on Diamonds Derived from Fuels, Division of Fuel Chemistry, ACS, 197th Meeting, Dallas, TX, April 9-14, 1989.

4. Presentation: "The Role of Ions in Soot Formation," at Flame Structure Seminar, Alma Alta, Soviet Union, September 1989.

5. Presentation: "Chemiionization," at AFOSR Workshop, June, 1989.

6. Presentation. "Large Ion Formation in a Sooting and Near Sooting Benzene/Oxygen Flame," at The Fall Technical Meeting, Eastern Section of the Combustion Institute, Orlando, FL, December, 1990.

7. Presentation: "Formation of Large Species in Sooting Flames by Free Radical and Ionic Mechanisms," at The Fall Technical Meeting, Eastern Section of the Combustion Institute, Orlando, FL, December, 1990.

During this period Prof. Phil Westmoreland and his student visited AeroChem to consult with us on their setting up a mass spectrometer to study flames. We have consulted with a number of people, including William Gardiner, Dave Golden, Sharon G. Lias, Steve Stein, and Phil Westmoreland from whom we have solicited help in setting up our mechanism.

XIII. INVENTIONS

None.

XIV. REFERENCES

1. Eraslan, A.N. and Brown, R.C., "Chemi-ionization and Ion-Molecule Reactions in Fuel-Rich Acetylene," Combust. Flame 74, 19 (1988).

2. Brown, R.C. and Eraslan, A.N., "Simulation of Ionic Structure in Clean and Close-to-Stoichiometric Acetylene Flames," Combust. Flame 73, 1 (1988).

3. Vovelle, C., Personal Communication, December 1989.

4. Frenklach, M. and Wang, H., "Computer Modeling of Soot Formation Comparing Free Radical and Ionic Mechanisms," Final Technical Report, January 22, 1991.

5. Calcote, H.F. and Keil, D.G., "Ion-Molecule Reactions in Sooting Acetylene-Oxygen Flames," Combust. Flame 74, 131 (1988).

6. Keil, D.G., Gill, R.J., Olson, D.B., and Calcote, H.F., "Ionization and Soot Formation in Premixed Flames," Twentieth Symposium (International) on Combustion (The Combustion Institute, Pittsburgh, 1985) p. 1129.

7. Keil, D.G., Gill, R.J., Olson, D.B., and Calcote, H.F., "Ion Concentrations in Premixed Acetylene-Oxygen Flames Near the Soot Threshold," in The Chemistry of Combustion Processes, T.M. Sloane, Ed., ACS Symposium Series 249 (American Chemical Society, Washington, DC, 1984) p. 33.

8. Bittner, J.D. and Howard, J.B., "Pre-Particle Chemistry of Soot Formation," in Particulate Carbon: Formation During Combustion, D.G. Siegla and G.W. Smith, Eds. (Plenum, New York, 1981) p. 109.

9. Calcote, H.F., Olson, D.B., and Keil, D.G., "Are Ions Important in Soot Formation?" Energy & Fuels 2, 494 (1988).

10. Rosenstock, H.M., Draxl, K., Steiner, B.W., Herron, J.T., J. Phys. Chem. Ref. Data 6, Suppl. 1 (1977).

11. Levin R.D. and Lias, S.G., "Ionization Potential and Appearance Measurements, 1971-1981," NSRDS-NBS 71 (1982).

12. Lias, S.G., Bartness, J.E., Liebman, J.F., Holmes, J.L., Levin, R.D., and Mallard, W.G., J. Phys. Chem. Ref. Data 17, Suppl. 1 (1988).

13. Calcote, H.F. and Gill, R.J., "Computer Modeling of Soot Formation Comparing Free Radical and Ionic Mechanisms," Annual Report, AeroChem TP-482, March 1989.

14. Westmoreland, P.R., "Importance of Obvious and Disguised Association Reactions in Combustion," submitted to J. Phys. Chem., September 1989.

15. Westmoreland, P.R., Personal communication on chemiionization, 9 October 1989.

16. Su, T. and Bowers, M.T., in Gas Phase Ion Chemistry, M. T. Bowers, Ed. (Academic Press, New York, 1979), Ch. 3.

17. Bates, D.R., "Density of Quantum States of Ion-Molecule Association Complex and Temperature Dependence of Radiative Association Coefficient," J. Chem. Phys. 73, 1000 (1980).

18. Bates, D.B., "Temperature Dependence of Ion-Molecule Association," J. Chem. Phys. 71, 2318 (1979).

19. Hwang, S.M., Gardiner, W.C., Jr., Frenklach, M., and Hidaka, Y., "Induction Zone Exothermicity of Acetylene Ignition," Combust. Flame 67, 65 (1987).

20. Cool, T.A. and Tjossem, J.H., "Direct Observation of Chemi-ionization in Hydrocarbon Flames Enhanced by Laser Excited $CH^*(A^2\Delta)$ and $CH^*(B^2\Sigma)$," Chem. Phys. Lett. 111, 82 (1984).

21. Chang, J.S. and Golden, D.M., "Kinetics and Thermodynamics for Ion-Molecule Association Reactions," J. Am. Chem. Soc. 103, 496 (1981).

22. Patrick, R. and Golden, D.M., "The Temperature Dependence of Ion-Molecule Association Reactions," J. Chem. Phys. 82, 75 (1985).

23. Dodds, J.A., Golden, D.M., and Brauman, J.I., "Entropy Bottlenecks in Ion-Molecule Reactions," J. Chem. Phys. 80, 1894 (1984).

24. Smith, D. and Adams, N.G., "Cyclic and Linear Isomers of $C_3H_2^+$ and $C_3H_3^+$: The $C_3H_2 + H_2$ Reaction," Int. J. Mass Spectr. Ion Proc. 76, 307 (1987).

25. Gioumousis, G. and Stevenson, D.P., "Reactions of Gaseous Molecule Ions with Gaseous Molecules. V. Theory," J. Chem. Phys. 29, 294 (1958).

26. Bockhorn, H., Fettig, F., and Wenz, H.W., "Investigation of the Formation of High Molecular Hydrocarbons in Premixed Hydrocarbon-Oxygen Flames," Ber. Bunsenges. Phys. Chem. 87, 1067 (1983).

27. Calcote, H.F., Kurzius, S.C., and Miller, W.J., "Negative and Secondary Ion Formation in Low Pressure Flames," Tenth Symposium (International) on Combustion (The Combustion Institute, Pittsburgh, 1965) p. 605.

28. Homann, K.H. and Stroefer, E., "Charged Soot Particles in Unseeded and Seeded Flames," in Soot in Combustion Systems, J. Lahaye and G. Prado, Eds. (Plenum Press, New York, 1981) p. 217.

29. Gerhardt, P. and Homann, K.H., "Ions and Charged Soot Particles in Hydrocarbon Flames. I. Nozzle Beam Sampling: Velocity, Energy, and Mass Analysis in Total Ion Concentrations," Combust. Flame 81, 289 (1990).

30. Sodha, M.S. and Guha, S., Adv. Plasma Phys. 4, 219 (1971).

31. Ogram, G.L., Chang, J.-S., and Hobson, R.M., "Dissociative Recombination of H_3O^+ and D_3O^+ at Elevated Electron and Gas Temperatures," Phys. Rev. 21, 982 (1980).

32. Griffin, G.W., Dzidic, I., Carroll, D.I., Stillwell, R.N., and Horning, E.C., "Ion Mass Assignments Based on Mobility Measurements," Anal. Chem. 45, 1204 (1973).

33. Hagen, D.F., "Characterization of Isomeric Compounds by Gas and Plasma Chromatography," Anal. Chem. 51, 870 (1980).

34. McDaniels, E.W., Collision Phenomena in Ionized Gases, (Wiley, New York, 1964) p. 512.

35. Smyth, K.C., Lias, S.G., and Ausloos, P., "The Ion Molecule Chemistry of $C_3H_3^+$ and the Implications for Soot Formation," Combust. Sci. Techn. 28, 147 (1982).

36. Baykut, G., Brill, F.W., and Eyler, J.R., "Reactions of $C_3H_3^+$ Ions with Aromatic Hydrocarbons and Alcohols and Their Implications for an Ionic Mechanism of Soot Formation," Combust. Sci. Techn. 45, 233 (1986).

37. Delfau, J.L., Michaud, P. and Barassin, A., Combust. Sci. Techn. 20, 165 (1979).

38. Frenklach, M. and Warnatz, J., "Detailed Modeling of PAH Profiles in a Sooting Low Pressure Acetylene Flame," Combust. Sci. Techn. 51, 265 (1987).

39. Frenklach, M. and Wang, H., "Detailed Modeling of Soot Particle Nucleation and Growth," Twenth-Third Symposium (International) on Combustion (The Combustion Institute, Pittsburgh. in press).

40. Frenklach, M., Clary, D.W., Gardiner, W.G., Jr., and Stein, S.F., "Detailed Kinetic Modeling of Soot Formation in Shock-Tube Pyrolysis of Acetylene," Twentieth Symposium (International) on Combustion (The Combustion Institute, Pittsburgh, 1984) p. 887.

41. Calcote, H.F., "Mechanisms of Soot Formation in Flames-A Critical Review," Combust. Flame 42, 215 (1981).

APPENDIX A

A Computer Code Designed for Modeling the Ionic Mechanism of Soot Formation

Robert C. Brown and Timothy W. Pedersen

Iowa State University

As a prerequisite for this study, it was necessary to develop a versatile computer code that could incorporate features that are not standard in reactive flow models. In particular, the code developed for this study can treat non-Arrhenius kinetics by use of a lookup table. The code also treats ionic mobility by calculating the electric field distribution throughout the flame region. Changes in reaction rates or reaction mechanisms were easily implemented into the computer code because of this versatility.

The reaction mechanism used in this study was separated into two models: a neutral species model and an ionic species model. This partition is based on the assumption that the ionic reactions do not change the neutral species and temperature profiles significantly. The neutral species profiles are treated as parameters in the ionic model.

Comparison of predicted and experimental neutral species profiles for rich acetylene flames demonstrated significant deficiencies in the present understanding of neu-

tral species mechanisms. Since this study focuses on ionic mechanisms of soot nucleation, we chose to use experimental profiles of neutral species as input to the ionic model. Furthermore, since the cyclic form of $C_3H_3^+$ is the starting ion for the proposed ionic mechanism, the experimental profile of this ion was also used as an input parameter to the ionic model, thereby circumventing the need for chemiionization reactions in the ionic model.

I. GOVERNING EQUATIONS

The equations describing a one–dimensional laminar premixed flame in the presence of an electric field include the mass and species conservation equations and Poisson's equation to describe the electric field intensity.

Mass conservation:

$$\frac{\partial \rho}{\partial t} + \frac{\partial(\rho u)}{\partial x} = 0 \tag{A.1}$$

Species conservation:

$$\rho \frac{\partial Y_i}{\partial t} + \rho u \frac{\partial Y_i}{\partial x} = -\frac{1}{A}\frac{\partial(AJ_i)}{\partial x} + \omega_i \tag{A.2}$$

where Y_i is the specie mass fraction and ω_i is the rate of chemical generation. The mass flux J_i is defined as

$$J_i = -D_{i,m}\rho \frac{\partial Y_i}{\partial x} + \mu_{i,m}\rho Y_i E. \tag{A.3}$$

The first term on the right side of the equation is the mass flux due to molecular diffusion and the second term is the mass flux due to ion mobility in the electric field. To avoid the use of ambipolar diffusion coefficients, a new method for calculating the mobility of ions in the presence of a self–induced electric field is used in this study. To

calculate the mass flux due to ion mobility, the electric field, E, is calculated directly from Poisson's equation:

$$\frac{d^2V}{dx^2} = -\frac{1}{\epsilon_o}(n_+ - n_-)e \tag{A.4}$$

where V is the voltage, ϵ_o is the permissivity constant, e is the electron charge, and n_+ and n_- are positive and negative ion concentrations, respectively.

The gas velocities for the flames in this research are on the order of 100 cm/s. The pressure throughout the flame is assumed to be nearly constant. Because of the small velocity and small pressure drop, the momentum equation does not need to be solved. Since an experimental temperature profile was used, there was no need to solve the energy equation.

To eliminate the convection terms from the conservation equations and to automatically satisfy continuity, a coordinate transformation [2] is made using

$$\frac{\partial \psi}{\partial x} = \rho \quad and \quad \frac{\partial \psi}{\partial t} = -\rho u. \tag{A.5}$$

The transformed equation for the ionic species mechanism is

$$\rho\frac{\partial \varphi}{\partial t} = \rho\frac{\partial}{\partial \psi}\left(\rho\Gamma\frac{\partial \varphi}{\partial \psi}\right) + \rho\frac{\partial}{\partial \psi}(\rho\Gamma') + G \tag{A.6}$$

where the expressions corresponding to Γ, Γ', and G are in Table A.1. The appropriate boundary conditions are

$$\varphi = \varphi_0 \quad at \quad \psi = 0 \tag{A.7}$$

and

$$\frac{\partial \varphi}{\partial \psi} = constant \quad at \quad \psi = \infty. \tag{A.8}$$

The variable φ is a generic term for Y_i and ψ is the transformed spatial variable.

Table A.1: Values of Γ, Γ' and G for the ionic species

Equation	Γ	Γ'	G
Species conservation	$D_{i,m}\rho$	$-\mu_{i,m}\rho Y_i E$	ω_i

Solving Equation (A.6) using the above boundary conditions gives the solution in the ψ–t coordinate system. A simple transformation back to the x–t coordinate system is obtained by a rearrangement of Equation (A.5),

$$x = \int_{\psi=0}^{\psi} \frac{d\psi}{\rho} \tag{A.9}$$

II. COMPUTATION METHOD

A. SOLUTION PROCEDURE

Solving Equations (A.6) numerically is difficult because of stiffness introduced by the chemical generation term G. This is due to the fact that G may vary by orders of magnitude in the problem domain. This problem can be circumvented by using the split operator technique [3] that will divide Equation (A.6) into two parts. The first part consists of the equation

$$\rho\frac{\partial\varphi'}{\partial t} = \rho\frac{\partial}{\partial\psi}\left(\rho\Gamma\frac{\partial\varphi'}{\partial\psi}\right) + \rho\frac{\partial}{\partial\psi}(\rho\Gamma'). \tag{A.10}$$

The second part is the equation

$$\rho\frac{\partial\varphi''}{\partial t} = G \tag{A.11}$$

where φ' and φ'' are dummy variables.

Equation (A.10) represents the time rate of change of φ due to transport and Equation (A.11) is the time rate of change of φ due to chemical generation.

Equations (A.10) and (A.11) are partial differential equations (PDEs) in time and space. Partial differential equations are by nature more difficult to solve than ordinary differential equations (ODEs). A system of ODEs would have the added advantage of using an ordinary differential equation solver in the solution process. The method of lines converts the system of PDEs to a system of ODEs [4]. This technique discretizes the spatial derivatives leaving a system of first order ODEs in time [2]. Central differencing of Equations (A.10) and (A.11) results in

$$\frac{d\varphi'_i}{dt} = \frac{1}{\Delta\psi^2}[\rho_{\frac{i+1}{2}}\Gamma_{\frac{i+1}{2}}(\varphi'_{i+1}-\varphi'_i)-\rho_{\frac{i-1}{2}}\Gamma_{\frac{i-1}{2}}(\varphi'_i-\varphi'_{i-1})] - \frac{\rho_{\frac{i+1}{2}}\Gamma'_{\frac{i+1}{2}}\varphi_{i+1}-\rho_{\frac{i-1}{2}}\Gamma'_{\frac{i-1}{2}}\varphi_{i-1}}{\Delta\psi_{i+1}+\Delta\psi_{i-1}}, \tag{A.12}$$

and

$$\frac{d\varphi_i}{dt} = \left(\frac{G}{\rho}\right)_i \tag{A.13}$$

for internal grid points, i=2,3,...N-1. The notations $\rho_{\frac{i+1}{2}}$, $\rho_{\frac{i-1}{2}}$, $\Gamma_{\frac{i+1}{2}}$ and $\Gamma_{\frac{i-1}{2}}$ are defined as

$$\rho_{\frac{i\pm1}{2}} = \frac{\rho_i+\rho_{i\pm1}}{2} \tag{A.14}$$

and

$$\Gamma_{\frac{i\pm1}{2}} = \frac{\Gamma_i+\Gamma_{i\pm1}}{2}. \tag{A.15}$$

The boundary conditions at $\psi = 0$ is described by

$$\frac{d\varphi_1}{dt} = 0. \tag{A.16}$$

The boundary condition at $\psi = \infty$ is described by

$$\frac{d\varphi_N}{dt} = \frac{2}{\Delta\psi^2}[\rho_{\frac{N-1}{2}}\Gamma_{\frac{N-1}{2}}(\varphi_N-\varphi_{N-1})] - \frac{2}{\Delta\psi}[\rho_{\frac{N-1}{2}}\Gamma'_{\frac{N-1}{2}}(\varphi_N-\varphi_{N-1})], \tag{A.17}$$

and

$$\frac{d\dot{\varphi}_N}{dt} = \left(\frac{G}{\rho}\right)_N \tag{A.18}$$

This results in 2N(NSPC+1) equations for NSPC chemical species and N nodes. The resulting system of equations is still computationally stiff due to the extreme differences in gas phase reactions rates. A special algorithm called TRANSEQI [2] was used to make the equations more tractable.

TRANSEQI was developed by Eraslan and Brown [2] to reduce stiffness of the differential equations describing reactive flow problems. In addition, core memory is reduced and a nonstiff ODE solver can be employed.

Estimated ionic species profiles are used as initial conditions in the algorithm. The transport coefficients and molar production rates are calculated for each specie at each nodal point based on these initial conditions. The transport equation for the first specie is solved holding the temperature and all other specie concentrations constant. At the next time step, the generation equation for the same specie is solved. The temperature and all other species concentrations are again held constant throughout the integration. The resulting $\Delta\varphi$ from the transport and chemical generation equations are added to the input φ. This gives the new φ value that is used in subsequent integrations. The transport and generation equations are then solved in the same manner for each of the remaining species. Property and mixture coefficients are then calculated using the new values of specie concentrations. The evaluation of property and mixture coefficients can be updated periodically rather than at the end of each time step, which helps reduce the number of computations executed in the program. This methodology is repeated until all time derivatives approach zero. Stiffness is virtually eliminated since only one specie is treated at any

one time by the integrator. Therefore, Euler's scheme and Gear's method are used to solve Equations (A.11) and (A.13) respectively.

To solve Poisson's equation (Eqn. A.4) it was rewritten in state variable form by defining the electric field intensity $E = -\frac{dV}{dx}$ and substituting into Equation (A.4):

$$\frac{dE}{dx} = \frac{1}{\epsilon_0}(n_+ - n_-)e \tag{A.19}$$

and

$$\frac{dV}{dx} = -E \tag{A.20}$$

with V(x=0) and V(x=L) at prescribed boundary conditions. The resulting boundary value problem was solved using a shooting method.

The predominate ion, cyclic $C_3H_3^+$, represents 99% of the total ion current. Since this ion is treated as an input parameter to the ionic model, Poisson's equation (Eqn. A.4) was only solved at the end of the first iteration in TRANSEQI. No further changes in the electric field are expected as long as the cyclic $C_3H_3^+$ profile remains fixed [5].

B. ESTIMATION OF INITIAL CONDITIONS

Good initial estimates of ion concentration profiles can result in substantial decreases in computation time. These initial profiles were obtained by neglecting transport effects and solving the resulting plug flow model described by

$$\frac{dY_i}{dx} = \frac{\omega_i}{\rho u}. \tag{A.21}$$

A value for the flame velocity, u, can be taken from experimental data for a given gas mixture equivalence ratio and pressure. These ionic species profiles were then used as initial conditions in Equations (A.11) and (A.13).

III. RESULTS

The results from the plug–flow model were compared to calculated ion profiles from Frenklach. When using Frenklach's neutral species profiles the plug–flow model calculated concentrations of major ions to within an order of magnitude of the values calculated by Frenklach's model. Both sets of calculated profiles exhibited peaks in concentrations which were much sharper than experimental. The calculated plug–flow ion concentrations were then used as initial conditions in the diffusion model which eliminated the sharp peaks by smoothing and broadening the profiles. Since the peak concentration did not change, it can be concluded that for this reaction mechanism, the plug flow model can be used to give good quantitative peak concentration values.

The use of ion–induced electric fields to calculate ion mobility did not significantly alter ion profiles compared to plug–flow calculations. Only if cyclic $C_3H_3^+$ becomes a variable in the model, rather than an input parameter, can ambipolar effects become apparent as ion profiles develop.

[1] Hunter, S. R. and Christophorou, L. G. "Electron Motion in Low- and High-Pressure Gases," *Electron-Molecule Interactions and Their Applications*. L.G. Christophorou ed. American Press, New York, 1984, 89-220.

[2] Eraslan, Ahmet N., and Brown, Robert C. "A Simple Iterative Procedure for Reducing Stiffness and Computer Memory in Reactive Flow Problems," *Computer Methods in Applied Mechanics and Engineering*, 64(1987): 61-77.

[3] Oran, Elaine S. and Boris, Jay P. "Numerical Simulation of Reactive Flow," Elsevier, New York, 1987.

[4] Madsen, N.K. and Sincovec, R.F. "The Numerical Method of Lines for the Solution of Nonlinear Partial Differential Equations," *Rept. OCRL-75142*, (1973).

[5] Conte, C.D. and de Boor, Carl "Elementary Numerical Analysis," McGraw-Hill, New York, 1980.